Nano-Micro Letters

e-ISSN 2150-5551
CN 31-2103/TB

REVIEW

https://doi.org/10.1007/s40820-023-01041-5

Cite as
Nano-Micro Lett.
(2023) 15:93

Received: 14 January 2023
Accepted: 22 February 2023

Nanostructuring of Mg-Based Hydrogen Storage Materials: Recent Advances for Promoting Key Applications

Li Ren[1], Yinghui Li[1], Ning Zhang[1], Zi Li[1], Xi Lin[1], Wen Zhu[1], Chong Lu[2], Wenjiang Ding[1], Jianxin Zou[1] ✉

HIGHLIGHTS

- A comprehensive discussion of the recent advances in the nanostructure engineering of Mg-based hydrogen storage materials is presented.
- The fundamental theories of hydrogen storage in nanostructured Mg-based hydrogen storage materials and their practical applications are reviewed.
- The challenges and recommendations of current nanostructured hydrogen storage materials are pointed out.

ABSTRACT With the depletion of fossil fuels and global warming, there is an urgent demand to seek green, low-cost, and high-efficiency energy resources. Hydrogen has been considered as a potential candidate to replace fossil fuels, due to its high gravimetric energy density (142 MJ kg^{-1}), high abundance (H_2O), and environmental-friendliness. However, due to its low volume density, effective and safe hydrogen storage techniques are now becoming the bottleneck for the "hydrogen economy". Under such a circumstance, Mg-based hydrogen storage materials garnered tremendous interests due to their high hydrogen storage capacity (~ 7.6 wt% for MgH_2), low cost, and excellent reversibility. However, the high thermodynamic stability ($\Delta H = -74.7$ kJ mol^{-1} H_2) and sluggish kinetics result in a relatively high desorption temperature (> 300 °C), which severely restricts widespread applications of MgH_2. Nano-structuring has been proven to be an effective strategy that can simultaneously enhance the ab/de-sorption thermodynamic and kinetic properties of MgH_2, possibly meeting the demand for rapid hydrogen desorption, economic viability, and effective thermal management in practical applications. Herein, the fundamental theories, recent advances, and practical applications of the nanostructured Mg-based hydrogen storage materials are discussed. The synthetic strategies are classified into four categories: free-standing nano-sized Mg/MgH_2 through electrochemical/vapor-transport/ultrasonic methods, nanostructured Mg-based composites via mechanical milling methods, construction of core-shell nano-structured

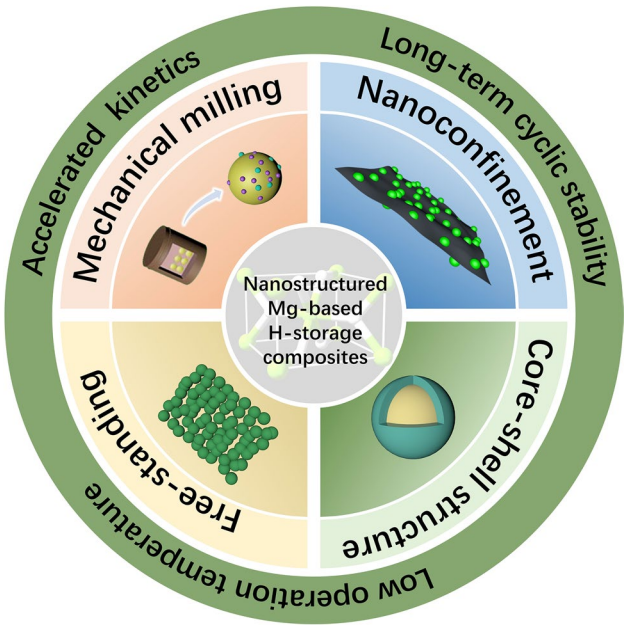

✉ Jianxin Zou, zoujx@sjtu.edu.cn
[1] National Engineering Research Center of Light Alloys Net Forming and State Key Laboratory of Metal Matrix Composites, Shanghai Engineering Research Center of Mg Materials and Applications and School of Materials Science and Engineering, Center of Hydrogen Science, Shanghai Jiao Tong University, Shanghai 200240, People's Republic of China
[2] Instrumental Analysis Center of SJTU, Shanghai Jiao Tong University, Shanghai 200240, People's Republic of China

Published online: 10 April 2023

Mg-based composites by chemical reduction approaches, and multi-dimensional nano-sized Mg-based heterostructure by nanoconfinement strategy. Through applying these strategies, near room temperature ab/de-sorption (< 100 °C) with considerable high capacity (> 6 wt%) has been achieved in nano Mg/MgH_2 systems. Some perspectives on the future research and development of nanostructured hydrogen storage materials are also provided.

KEYWORDS Mg-based hydrogen storage materials; Nanostructure; Hydrogen storage; Thermodynamics; Kinetics; On-board hydrogen storage

1 Introduction

In recent decades, the energy crisis and global warming have promoted a growing demand for renewable clean energy [1, 2, 3]. As a clean and sustainable energy resource, hydrogen (H_2) has been hailed as a future fuel that holds great promise in replacing ever-being-exhausted fossil fuels and aiding the transition to net-zero emissions [4, 5]. Hydrogen is the most abundant element in the universe and its combustion produces only water [6, 7, 8]. However, many obstacles need to be overcome to realize the so-called "hydrogen economy". The usage of hydrogen energy includes hydrogen production, hydrogen storage, hydrogen transportation, and hydrogen utilization. As known, the main challenge for the applications of hydrogen energy is the development of suitable approaches for hydrogen storage [9].

Economic, efficient, and safe hydrogen storage methods play a crucial role in exploiting hydrogen energy, reducing carbon emissions, and improving the utilization efficiency of renewable clean energies [10]. Compressed gaseous hydrogen storage technologies have long taken a dominant position in this field due to their simple, convenient, low energy consumption, and efficient advantages [11]. However, high-pressure gaseous hydrogen storage technology has the disadvantage of low volumetric hydrogen storage density and the safety risk of leakage and explosion. Cryogenic liquid hydrogen storage is limited by high cost and energy consumption [12]. Solid-state hydrogen storage in hydrides has been considered as a promising hydrogen storage technology [13]. Although the industrial application of solid-state hydrogen storage technologies with metal hydride is still in the stage of an attack. Metal hydride-based hydrogen storage method can effectively overcome the shortcomings rising from other hydrogen storage techniques, and it is suitable for fuel cell vehicles due to its high volumetric hydrogen storage density, easy operation, convenient transportation, low cost, and high safety [14, 15, 16].

Among numerous hydrides, magnesium hydride (MgH_2) has received wide attention by virtues of its high gravimetric (7.6 wt% H_2) and volumetric (110 kg H_2 m^{-3}) hydrogen storage capacity, abundant reserve, and environmental friendliness [17]. However, the implementation of MgH_2 as a hydrogen-storage medium has long been restricted by two dominating intrinsic challenges, the first obstacle is the high thermodynamic stability ($\Delta H = 74.7$ kJ mol^{-1} H_2) resulting in the high decomposition temperature of MgH_2. The desorption enthalpy for MgH_2 should be tailored into the range of 42–55 kJ mol^{-1} H_2, if the Mg/MgH_2 releases hydrogen near 1 bar and fuel-cell operating temperatures (50–150 °C) [18, 19]. Another obstacle is the rather sluggish hydrogen ab/de-sorption kinetics originating from high H_2 dissociation energy barrier, slow hydrogen diffusion rate in MgH_2 bulk, etc. [20]. As early as 1951, MgH_2 was first synthesized by direct reaction of Mg and H_2. In the past decades, great efforts have been devoted to the development of Mg-based hydrogen storage composites with fast kinetics, low operation temperature, high reversible capacity, long cycling life, low cost, and high safety, as landmarked by the application of alloying [21, 22, 23, 24, 25, 26], nanostructuring [27, 28, 29, 30, 31], and catalyzing [32, 33, 34, 35, 36]. Alloying is a simple and mature method to modify Mg/MgH_2. By adding alloying elements to the Mg/MgH_2 system to change its hydrogen ab/de-sorption reaction paths, the thermodynamic properties of MgH_2 can be effectively improved. In 1968, Reilly et al. [37] first discovered that the intermetallic compound Mg_2Ni, formed by introducing the alloying element Ni into Mg/MgH_2 system, presented excellent hydrogen ab/de-sorption thermodynamic performances. Subsequently, Fe, Co, Si, Cu, and other alloying elements were also introduced into Mg/MgH_2 system to investigate the hydrogen storage properties of their corresponding alloy compounds. However, the biggest drawback of alloying is that the introduction of alloying elements will lead to capacity loss, and some Mg-based hydrogen storage alloys exhibit

 https://doi.org/10.1007/s40820-023-01041-5

an irreversible hydrogen ab/de-sorption process. Additionally, it is worth emphasizing that MgH_2 is a semiconductor with no available electronic states at the Fermi level [38], having almost no catalytic activity toward H_2 surface reactions. In contrast, The Fermi level of transition metals is located around *s*-type orbitals, which is a necessary condition to promote H_2 surface reactions [39]. Hence, catalyzing has been a widely studied and efficient method to improve the hydrogen storage kinetics of MgH_2 since the 1990s. The scope of these catalysts extends from transition metals to transition metal oxides, halides, and carbides. In addition to the catalyzing, the preparation of hydrogen storage composites by compounding complex hydrides with MgH_2 is also a hot research topic in recent years [40, 41]. Although the alloying and catalyzing could indeed ameliorate the performances of MgH_2 from the extrinsic perspective, the improvement is restricted by the inevitable agglomeration and growth of the additives during cycling, as well as the low density of exposed active sites. Hence, from an intrinsic point of view, nano-sized MgH_2 has been widely studied through various nanotechnologies giving rise to improved hydrogen storage performances of MgH_2 in recent years.

Based on the above discussions, nano-structuring has been regarded as one of the most efficient methods to destabilize MgH_2 and minimize the decomposition enthalpy among various modification strategies [42, 43]. Nano-sized materials have peculiar properties that could not be expected in the bulk phase. The surface layer atoms of nano-sized materials in the sub-stable state with high surface energy are highly susceptible to combining with other atoms and converting to the stable state, due to the presence of a large number of unsaturated bonds [44, 45]. It is worth emphasizing that the essence of the hydrogen ab/de-sorption process of Mg-based hydrogen storage composites is the bonding and breaking of Mg and H atoms, the nanosizing of MgH_2 has promising applications in the improvement of thermodynamics and kinetics of Mg-based hydrogen storage materials. Furthermore, it is important to distinguish between grain size, particle size, and crystal size in order to accurately describe the effects of each factor on the kinetics and thermodynamics of MgH_2. The particle size refers to the size of individual particles of a material. The particle size of MgH_2 can affect its thermodynamics and kinetics by altering the surface area-to-volume ratio. In general, smaller particles have a larger surface area-to-volume ratio than that of larger particles, which can enhance the reactivity and reaction rate of MgH_2 by increasing the number of active sites available for de/re-hydrogenation. The crystal size of MgH_2 refers to the size of individual crystals in a material. When MgH_2 is in a crystalline state, the size of the crystals can impact the nucleation and growth of new phases, as well as the overall crystal structure of the material, which can affect the reaction kinetics and thermodynamics. In general, smaller crystal sizes can promote faster nucleation and growth of new phases, as well as increase the number of defects and grain boundaries that can serve as reaction sites. Furthermore, the downsizing of the MgH_2/Mg crystal leads to a change in the lattice, which will result in a change in desorption energy via the changed lattice energies, thereby destabilize MgH_2. The grain size of MgH_2 is related to the crystal size, but refers specifically to the size of the individual grains in a polycrystalline material. In the case of MgH_2, smaller grains can provide a greater surface area, more nucleation sites, and shorter diffusion path for hydrogen absorption and desorption, similar to smaller crystal sizes. Thus, the main reasons for the amelioration of the hydrogen storage properties of Mg-based materials by nanosizing are as follows:

(a) With the increase of the specific surface area of nano-sized MgH_2, the contact area between the matrix and hydrogen is increased, accelerating the diffusion rate of hydrogen to the matrix. Besides, the contact area between the MgH_2/Mg and catalysts is also increased, improving catalytic efficiency.
(b) With the nanosizing of MgH_2, the surface energy increases, facilitating the adsorption of H_2 on the surface of Mg particles and the destabilization of MgH_2.
(c) The high density of grain boundaries among nanoparticles provides more diffusion paths for hydrogen atoms, improving the hydrogen storage kinetics of MgH_2.
(d) Reducing the size of MgH_2 effectively shortens the diffusion path of hydrogen, enhancing the kinetic properties of MgH_2/Mg.

The preparation methods of nano-sized Mg-based hydrogen storage materials include ball-milling, vapor deposition method, plasma metal reaction, chemical reduction of Mg precursors, and nanoconfinement. Many high-quality reviews have been published in the last decade covering the thermal destabilization and catalytic tuning of

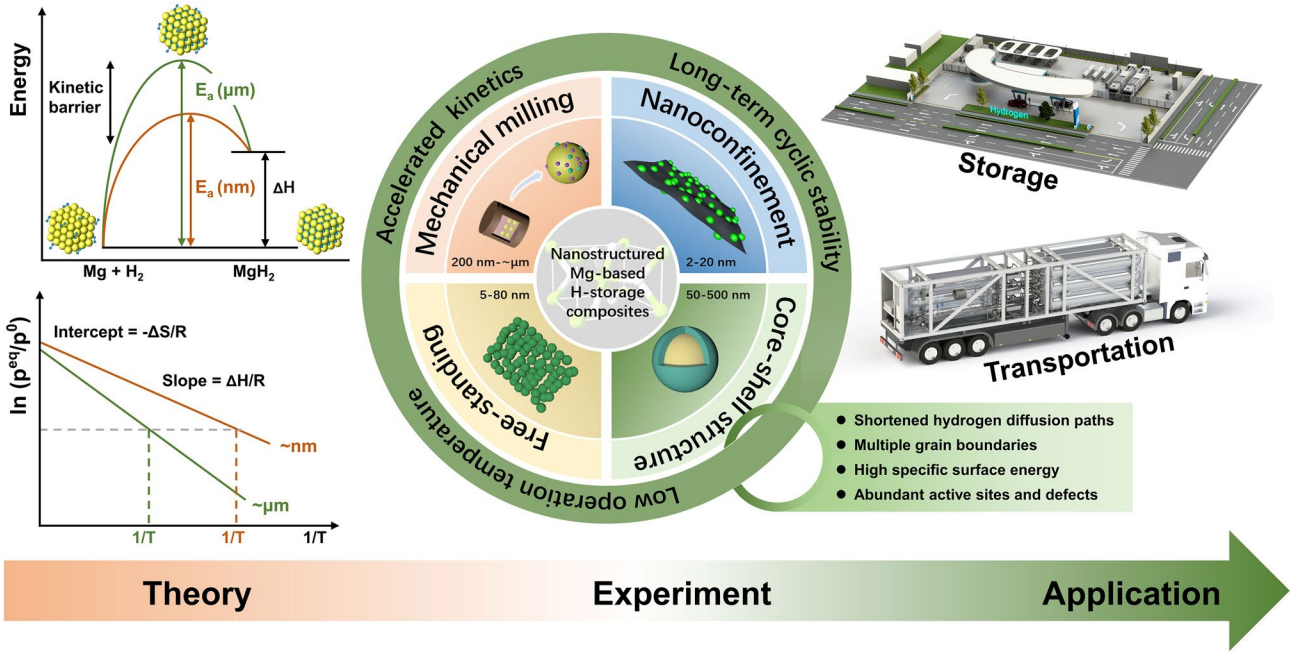

Scheme 1 Schematic illustrations of fundamental theories and synthetic strategies for nano-engineering of Mg-based hydrogen storage materials

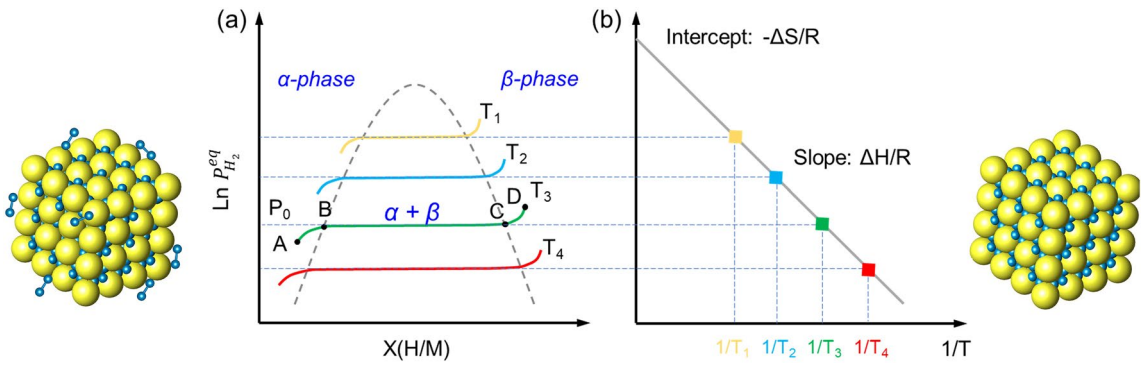

Fig. 1 **a** Pressure–composition isotherm plot of Mg + H_2 ⇄ MgH_2 transition. **b** van't Hoff plot related to the phase transition of Mg + H_2 ⇄ MgH_2. The enthalpy and entropy of hydrogenation and dehydrogenation could be obtained from the slope and intercept, respectively. Schematic representations of the α-phase (left) and β-phase (right) of metal hydride are also presented

the kinetics of Mg-based hydrogen storage materials [14, 20, 46, 47]. However, a specific focus on nanostructure engineering of Mg-based hydrogen storage materials is still missing and necessary for their applications in future energy storage.

Herein, we make great efforts to present a comprehensive overview of fundamental theory and synthetic methodologies for intricate nanostructured Mg-based hydrogen storage composites, as depicted in Scheme 1. The fundamental theories of hydrogen storage regarding MgH_2 are highlighted with special emphasis on thermodynamics, kinetics, and cycling stability. This review paper summarizes the latest trends in the design of nanostructured Mg-based hydrogen storage materials, important breakthroughs in the field, and the challenges for Mg-based composites applied in the commercial energy conversion and storage devices.

https://doi.org/10.1007/s40820-023-01041-5

2 Fundamental Theories of Hydrogen Storage in MgH_2

2.1 Thermodynamics and Destabilization of the Mg/MgH_2 System

The hydrogen ab/de-sorption process of hydrides is a dynamic equilibrium of three phases: hydrogen, metal, and the corresponding hydride (Fig. 1). As shown in Fig. 1a, hydrogen pressure, composition, and temperature are the crucial factors determining the phase equilibrium [48]. During the process of isothermal hydrogenation, a solid solution (α-phase) is first formed. With the increase of hydrogen pressure, the solid solution starts to transform into hydride (β-phase), the β-phase nucleates and grows, and the hydrogen pressure remains unchanged as the phase transformation proceeds. Until the α-phase completely transforms to the β-phase, the hydrogenation reaction completes. By calibrating the pressure–composition–temperature equilibrium point in the process of hydrogen ab/de-sorption, the PCT curve can be obtained (Fig. 1b). The relationship between plateau pressure (P_{eq}) and temperature (T) in the PCT curve can be described by the van't Hoff equation:

$$\ln\left(\frac{P_{eq}}{P_0}\right) = \frac{\Delta H}{RT} - \frac{\Delta S}{R} \tag{2-1}$$

In this formula, P_0 is the atmospheric pressure (1.01×10^5 Pa); ΔH and ΔS are the enthalpy and entropy of the hydrogen ab/de-sorption, respectively; and T is the absolute temperature; R is the gas constant ($R = 8.314$ J mol^{-1} K^{-1}). According to the linear fitting between ln$P$ and 1000/T, ΔH and ΔS can be calculated. Notably, the value of the re/de-hydrogenation enthalpy (ΔH) is an important indicator to measure the strength of the Mg–H bond. The larger the absolute value of ΔH is, the stronger the Mg–H bond will be.

The thermodynamic stability of Mg/MgH_2 system is mainly determined by the feature of the Mg–H bond. The Mg–H bond in the Mg/MgH_2 system is covalent–ionic mixed [49], having a relatively high bonding energy of around 3.35 eV. The nature of Mg–H bond results in a high enthalpy for the decomposition of MgH_2, which is around 74.7 kJ for releasing 1 mol of H_2 [50], leading to a high temperature for hydrogen desorption. Under atmospheric pressure, MgH_2 starts to release H_2 at a temperature of 280 °C, which is far from the requirements of practical applications [51]. Many efforts have been made to thermodynamically destabilize the Mg/MgH_2 systems, such as alloying of Mg with other elements, inducing the formation of metastable γ-MgH_2 phase, and nano-structuring [52]. Cheung et al. [53] simulated the relationship between grain size reduction and decreased structural stability. They concluded that significant changes in the thermodynamics of hydrogen desorption are observed only if the grain size is reduced to below 2 nm.

2.2 Kinetics of the Mg/MgH_2 System

The thermodynamic parameters of the hydrogen storage materials characterize the driving force of phase transformation during hydrogen absorption and desorption. While hydrogen storage performances of the hydrides are also related to the re/de-hydrogenation rate, i.e., the kinetic properties.

The hydrogenation process of Mg includes four main steps: H_2 physisorption, H_2 dissociation, H chemisorption, and H atom diffusion [55]. Each step needs to overcome an energy barrier, called the reaction activation energy (Fig. 2). The relevant experiments have revealed that the rate-determining step is the nucleation-growth of MgH_2, which is determined by the hydrogen diffusion rate in Mg lattice [56]. However, the diffusivity of hydrogen in Mg lattice is quite low, which is measured to be 10^{-20} m^2 s in bulk Mg and 10^{-18} m^2 s along grain boundaries [57, 58]. It is worth emphasizing that the firstly formed MgH_2 will act as a barrier to further diffusion of hydrogen into bulk Mg, limiting the reaction rate of the hydrogenation process [59]. The hydrogen desorption of MgH_2 is mainly determined by the breakage of Mg–H bonds, diffusion of hydrogen atoms in the bulk phase, and recombination of hydrogen atoms. Accordingly, it is demonstrated that the sluggish kinetics (160 kJ mol^{-1} H_2) severely limits the wide application of Mg/MgH_2 system. Particularly, in the dehydriding stage of coarse particles, successively formed fresh Mg at the surface layer may function as the diffusion barrier to the hydrogen escaping from MgH_2. However, in nano-sized MgH_2 particles, the Mg phase may form

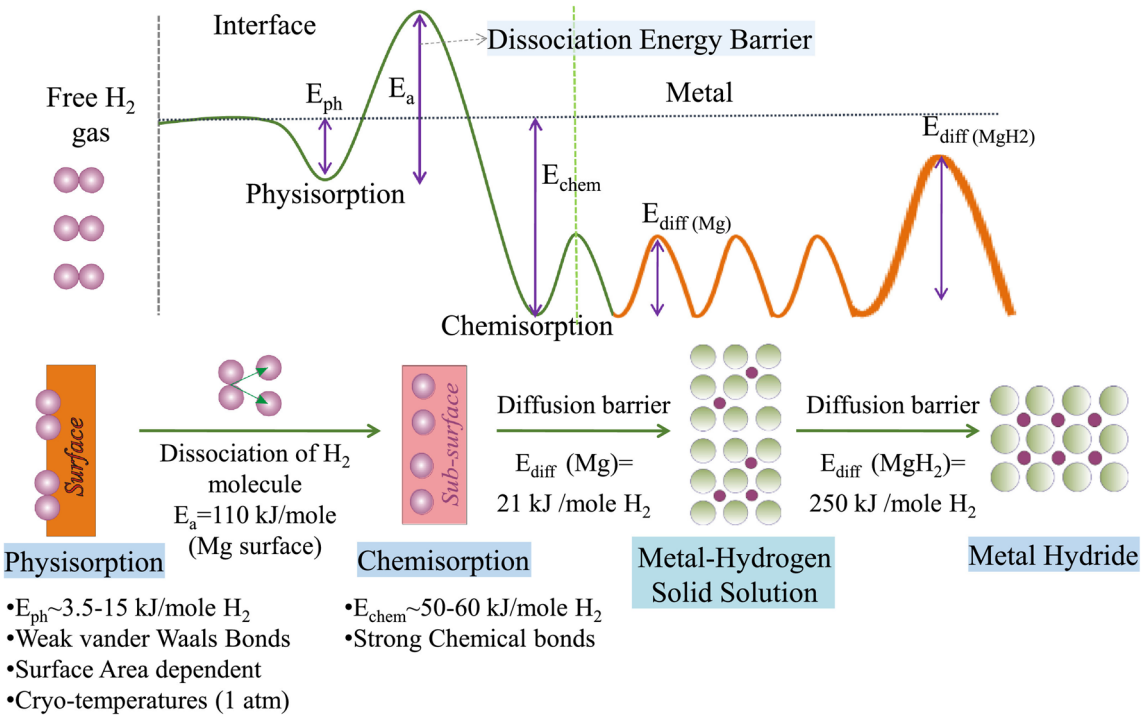

Fig. 2 Schematic diagram describing continuous energy barriers in the process of hydrogen absorption (up) and illustration of the kinetic steps in the hydrogen storage process (down). Reproduced with permission from Ref. [54]. Copyright 2021 Elsevier

Table 1 Kinetic models for hydrogen absorption and desorption process

Model equation	Description
$\alpha = kt$	
$[-\ln(1-\alpha)]^{1/n} = kt$	JMAK model n = 3, three-dimensional nucleation and growth mode n = 2, two-dimensional nucleation and growth mode
$1 - \ln(1-\alpha)^{1/n} = kt$	Shrinking core model n = 3, three-dimensional nucleation and growth mode n = 2, two-dimensional nucleation and growth mode
$1 - \left(\frac{2\alpha}{3}\right) - (1-\alpha)^{\frac{1}{3}} = kt$	Shrinking core model Three-dimensional growth process of the nucleus is controlled by the diffusion process Slowed growth rate of the grain boundary interface affects the growth rate of the nucleus

simultaneously all through the material and the entire process of desorption is then governed by fast hydrogen diffusion rather than slow Mg–MgH_2 boundary movement. In other words, particle size of MgH_2 has a profound effect on its hydrogen storage kinetic properties [60, 61].

To understand the mechanism of reaction kinetics, it is necessary to analyze kinetic models in the process of hydrogen ab/de-sorption. The kinetic models of hydrogen storage materials in the process of de/re-hydrogenation can be summarized in Table 1 [62, 63, 64].

Among them, the hydrogen ab/de-sorption process of most hydrogen storage materials can be described by the nucleation and growth mechanism (JMAK model), and the equation is as follows [65]:

$$\ln[-\ln(1-\alpha)] = n\ln k + n\ln t \quad (2\text{-}2)$$

In this formula, k is the rate constant of hydrogen ab/de-sorption; α is the reaction fraction corresponding to t; n is the dimension determining the abstract model. By establishing the linear relationship between $\ln[-\ln(1-\alpha)]$ and $\ln t$, the value of n can be obtained from the slope, and the reaction rate constant of k can be calculated by the intercept.

https://doi.org/10.1007/s40820-023-01041-5

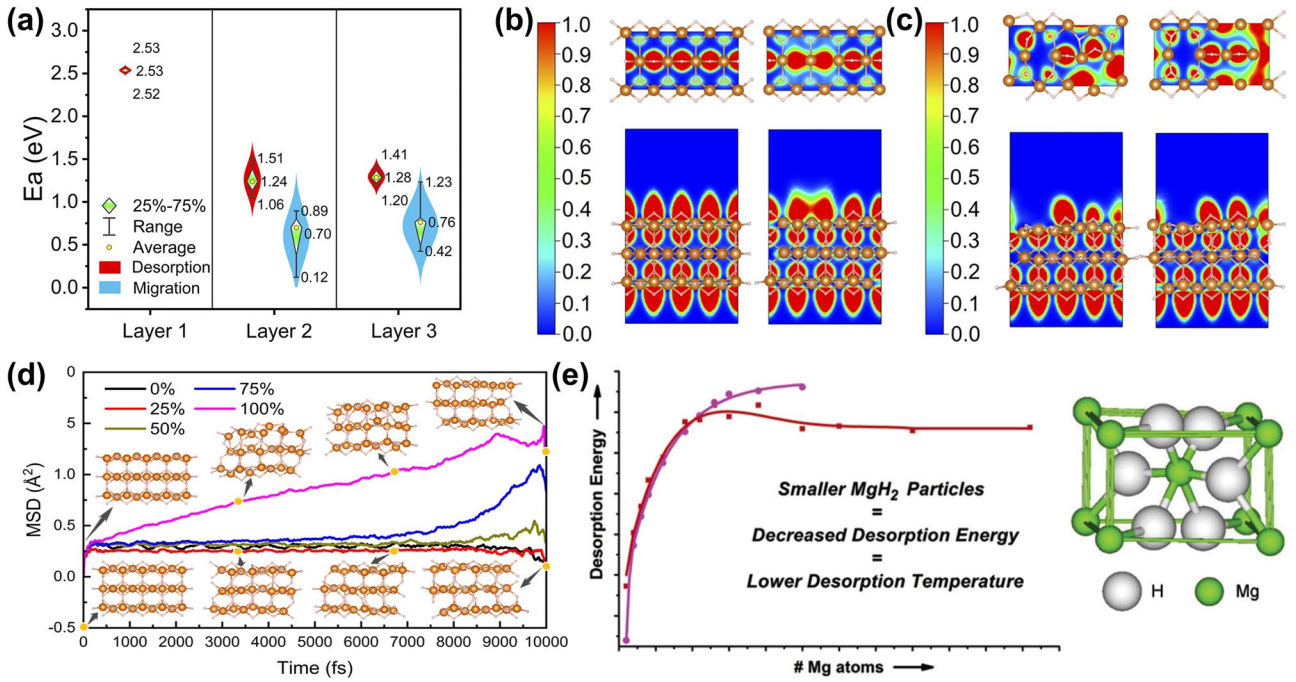

Fig. 3 **a** Comparison of the three-layer atomic H migration and dehydrogenation energy barriers. The calculated ELFs of MgH_2 before the dehydrogenation **b** in processes 1 and 2 (the first layer) and **c** in processes 3 and 4 (the second layer). **d** AIMD simulations on MgH_2 (110) before and after surface H loss. Yellow dots are the selected points of MgH_2 before (0%) and after (100%) surface H loss at 500 K. White and orange spheres represent H and Mg, respectively. Reproduced with permission from Ref. [19]. Copyright 2022 Royal Society of Chemistry. **e** Calculated desorption energies for MgH_2 clusters with both the HF method and DFT method. Reproduced with permission from Ref. [68]. Copyright 2005 American Chemical Society. (Colour figure online)

Furthermore, the activation energy (E_a) of hydrogen storage materials in the process of hydrogen ab/de-sorption can be obtained through the Arrhenius formula [66]:

$$k = Ae^{-\frac{E_a}{Rt}} \tag{2-3}$$

$$\ln k = -\frac{E_a}{RT} + \ln A \tag{2-4}$$

In which k is the rate constant, A is the pre-exponential factor, and E_a is the activation energy. Thus, the activation energy can be obtained by fitting ln$k$ verses $1/T$ [the reaction rate constants of k at different temperatures can be calculated from Eq. (2-2)]. The intrinsic mechanism of the hydrogen ab/de-sorption kinetic properties of materials can then be explained from the perspective of activation energy.

Moreover, Kissinger's method is also usually used to calculate the dehydrogenation activation energy of hydride, typically using differential scanning calorimetry (DSC) experiments, following Kissinger's equation [66, 67]:

$$\ln\left(\frac{\beta}{T_p^2}\right) = -\frac{E_a}{RT_p} + C \tag{2-5}$$

In this formula, β is the heating rate; T_p is the peak temperature; R is the gas constant ($R = 8.314$ J mol^{-1} K^{-1}); C is a constant. By fitting the linear relationship between $\ln\left(\frac{\beta}{T_p^2}\right)$ and $1000/T_p$, the activation energy (E_a) can be obtained using DSC results at different heating rates. Kissinger's method has advantages of being simple and requiring few tests. However, only a single rate-limiting step is assumed, the application of the equation is limited.

Dong et al. [19] studied the sequential MgH_2 dehydrogenation mechanism by analyzing the kinetic and structural changes during the layer-by-layer hydrogen desorption process through spin-polarized density functional theory calculations with van der Waals corrections (DFT-D3). The results showed that initial dehydrogenation barriers (2.52 and 2.53 eV) were much higher than the subsequent

reaction barriers (0.12–1.51 eV) (Fig. 3a). Moreover, after the desorption of all surface atomic H, the degree of electron localization in this region dropped sharply, resulting in a burst effect (Fig. 3b, c). The results of AIMD simulations indicated that after the loss of all the surface atomic H, the atomic H of MgH_2 was inclined to diffuse, and therefore, the dehydrogenation kinetics could be significantly improved (Fig. 3d), which inspired us the importance of promoting the initial dehydrogenation by structural engineering (such as nanostructure engineering) to facilitating the hydrogen desorption of MgH_2. It was also demonstrated that the desorption energy of MgH_2 decreased as the cluster size was reduced to below 19 Mg atoms [68]. For the smallest possible cluster, the desorption energy of MgH_2 dropped even to negative values, which means that the nanostructure engineering makes MgH_2 unstable (Fig. 3e).

Compared with the improvement in thermodynamics, the kinetic properties of Mg/MgH_2 can be adjusted more easily and effectively. Numerous strategies are effective in improving kinetic performance, such as alloying, catalyzing, nano-structuring, etc., which will be discussed in the following sections.

2.3 Cycling Stability of the Mg/MgH_2 System

Long-term cycling stability also plays a decisive role in the application of Mg-based hydrogen storage composites. The experimental results show that the long-term re/de-hydrogenation cycle at high temperatures will deteriorate the hydrogen storage capacity and the hydrogen ab/de-sorption rate [43, 69, 70, 71]. The reasons for the degradation of the system can be attributed to the following two factors. On one hand, the passivation of the Mg/MgH_2 interface resulted from the reaction between Mg/MgH_2 and contamination gas in H_2, causing the loss of capacity [72]. On the other hand, the agglomeration and growth of nanoparticles driven by the interfacial energies increase the diffusion pathway for hydrogen and deteriorate the kinetics of Mg/MgH_2 systems.

To improve the cyclic stability, apart from using purified H_2 to prevent capacity loss, the nanoconfinement and encapsulation strategy are effective methods to restrict the agglomeration and growth of nanoparticles. The research of nanoconfinement will be discussed in detail in the following section.

3 Tuning the Properties of the Mg/MgH_2 System Through Nanotechnology

The destabilization of MgH_2 by nano-structuring has been widely investigated both theoretically and experimentally. As the size of particles reduces to nanoscale, the surface energy cannot be ignored. Due to the extra interfacial free energy stored at the boundary, the hydrogen ab/de-sorption temperature will be decreased, indicating that Mg-based hydrogen storage materials can be substantially destabilized by inducing nanocrystalline structure [73]. The equilibrium pressure of nano-sized MgH_2 particles and corresponding bulk MgH_2 during the hydrogen desorption process obeys the following relationship [51]:

$$\ln\frac{P_{nano}^{eq}}{P_{bulk}^{eq}} = \frac{1}{RT}\left(\frac{3V_{Mg}\gamma_{Mg}}{r_{Mg}} - \frac{3V_{MgH_2}\gamma_{MgH_2}}{r_{MgH_2}}\right) \quad (3\text{-}1)$$

In this formula, P_{nano}^{eq} and P_{bulk}^{eq} are equilibrium pressures of nanoparticles and corresponding bulk, respectively; V is molar volume; γ is the surface energy density; r is radius of the spherical particle. It can be deduced that part of the formation enthalpy will be stored as excessive surface energy when the contribution of the size effect becomes sufficiently large, resulting in the destabilization of the MgH_2 nanoparticles. Particularly, as a typical phase transformation, the hydrogen ab/de-sorption process first takes place along the interface region, thus interfacial energy plays a crucial role in tuning the hydrogen storage performance. The formation of nanocrystalline with high density of interfaces will induce high extra energy stored in the interfacial region, which can reduce the energy barrier of de/re-hydrogenation [73, 74].

Thus, nano-structuring can significantly reduce the hydrogen ab/de-sorption temperature and increase the rate of re/de-hydrogenation of MgH_2, due to the introduction of defects, shortening of hydrogen diffusion paths, increasing of nucleation sites, and destabilization of Mg–H bonding. However, due to the high surface energy, nanoparticles are susceptible to agglomeration and growth. It is essential for exploring an appropriate strategy to prepare Mg-based nanostructured composites. In the following sections, we will review the synthesis methods of nanostructured Mg-based hydrogen storage materials in detail.

https://doi.org/10.1007/s40820-023-01041-5

3.1 Synthesis of Free-Standing Nano-sized Mg/MgH_2

Wagemans et al. [68] theoretically investigated the influence of crystal grain size on the thermodynamic stability of Mg/MgH_2. The results showed that both MgH_2 and Mg become less stable with the decreasing of cluster size and the absolute value of enthalpy reduced dramatically when crystallite sizes were decreased down to less than 1.3 nm. Particularly, a lower decomposition enthalpy of 63 kJ mol^{-1} H_2, corresponding to a desorption temperature of only 200 °C at 1 bar hydrogen pressure, may be obtained for 0.9 nm sized MgH_2 crystallites. They indicated that the downsizing of the MgH_2/Mg caused a change in the lattice, thus resulting in the reduction of desorption energy via the changed lattice energies. Impressively, they found that nano-sized Mg possessed the potential to uptake a few additional percent of hydrogen above the stoichiometric MgH_2 through a stepwise calculation on the hydrogen sorption processes. The extra hydrogen (10-15%) was not dissociated and adsorbed to the surface of MgH_2 as hydrogen molecules, depending on the specific surface area of nano-sized MgH_2, which was rare in bulk systems. It is worth emphasizing that "excess" hydrogen is less strongly bound to the MgH_2 structure and can therefore be desorbed at lower temperatures. Their quantum chemical study inspires us that it is possible to prepare MgH_2 clusters that can adsorb extra hydrogen molecules on the surface due to its unique nano-structure, which will release hydrogen at lower temperatures, and is suitable for the operation of proton exchange membrane fuel cell (PEMFC). While the waste heat released by the PEMFC can be used for the dehydrogenation of stoichiometric MgH_2, thereby achieving maximum energy utilization. However, these assumptions are simply not possible in bulk materials.

Experimentally, preparation of Mg/MgH_2 nanoparticles seems to be difficult, due to the high reactivity of Mg. In 2008, Aguey-Zinsou et al. [75] successfully prepared surfactant-stabilized Mg nanoparticles with an average diameter of 5 nm through electrochemical synthesis, which exhibited unique hydrogen storage properties (Fig. 4a). Almost all hydrogen could desorb from colloidal MgH_2 at a low temperature of 85 °C. This was the first time that hydrogen desorption near room temperature was achieved by nanosized MgH_2. Except for MgH_2/Mg nanoparticles, Chen et al. innovatively reported the non-confined Mg nanoparticles with different morphologies (nanowires, nanoflakes, nanorods, and sea-urchin-like shapes) via a vapor-transport method, which displayed enhanced hydrogen-sorption kinetics (Fig. 4b) [76, 77]. However, unsatisfactorily, the minimum diameter of these nano-sized Mg was larger than 30 nm. Mg nanocrystals of controllable sizes smaller than 30 nm were successfully synthesized in gram quantities by Norberg et al. [44] through chemical reduction of magnesocene using a reducing solution of potassium (Fig. 4c). The prepared Mg nanocrystals with smaller diameters exhibited dramatically faster hydrogen sorption kinetics, attributed to the reduction of particle size and increase of the defect density.

However, unfortunately, it is difficult to synthesize free-standing ultrafine MgH_2 nanoparticles (< 10 nm) due to their high surface energy, strong reduction trend, and high water–oxygen sensitivity. The particle size of MgH_2 synthesized by the methods mentioned above is generally large (> 30 nm) and the improvements in hydrogen storage performance are limited, unable to meet the requirements of practical applications. Recently, Zhang et al. [78] synthesized non-confined ultrafine MgH_2 nanoparticles (4–5 nm) by the metathesis process of liquid–solid phase driven by ultrasound (Fig. 4d). The ultrasound was used to provide the driving force for the formation of MgH_2, while combining the mechanical oscillation generated by ultrasound to inhibit the agglomeration of particles. A reversible hydrogen storage capacity of 6.7 wt% at 30 °C was achieved, bringing MgH_2 a step closer to practical applications. Furthermore, the results of DFT calculations revealed that the reaction barrier for the decomposition of nano-sized MgH_2 was remarkably lower than that of bulk MgH_2 (Fig. 5), indicating that nanostructure engineering of MgH_2 is thermodynamically and kinetically favorable to the enhanced performance.

3.2 Preparation of Nanostructured Mg-Based Composites via Mechanical Milling

Mechanical milling plays a significant role in the field of energy storage and conversation, such as batteries, catalysis and hydrogen energy. Particularly, ball-milling has been proven to be a facile method to prepare Mg-based composites in hydrogen storage fields. It has been found that the MgH_2 and catalysts with various morphologies and compositions can be mixed evenly to form nanostructured Mg-based composites through the simple

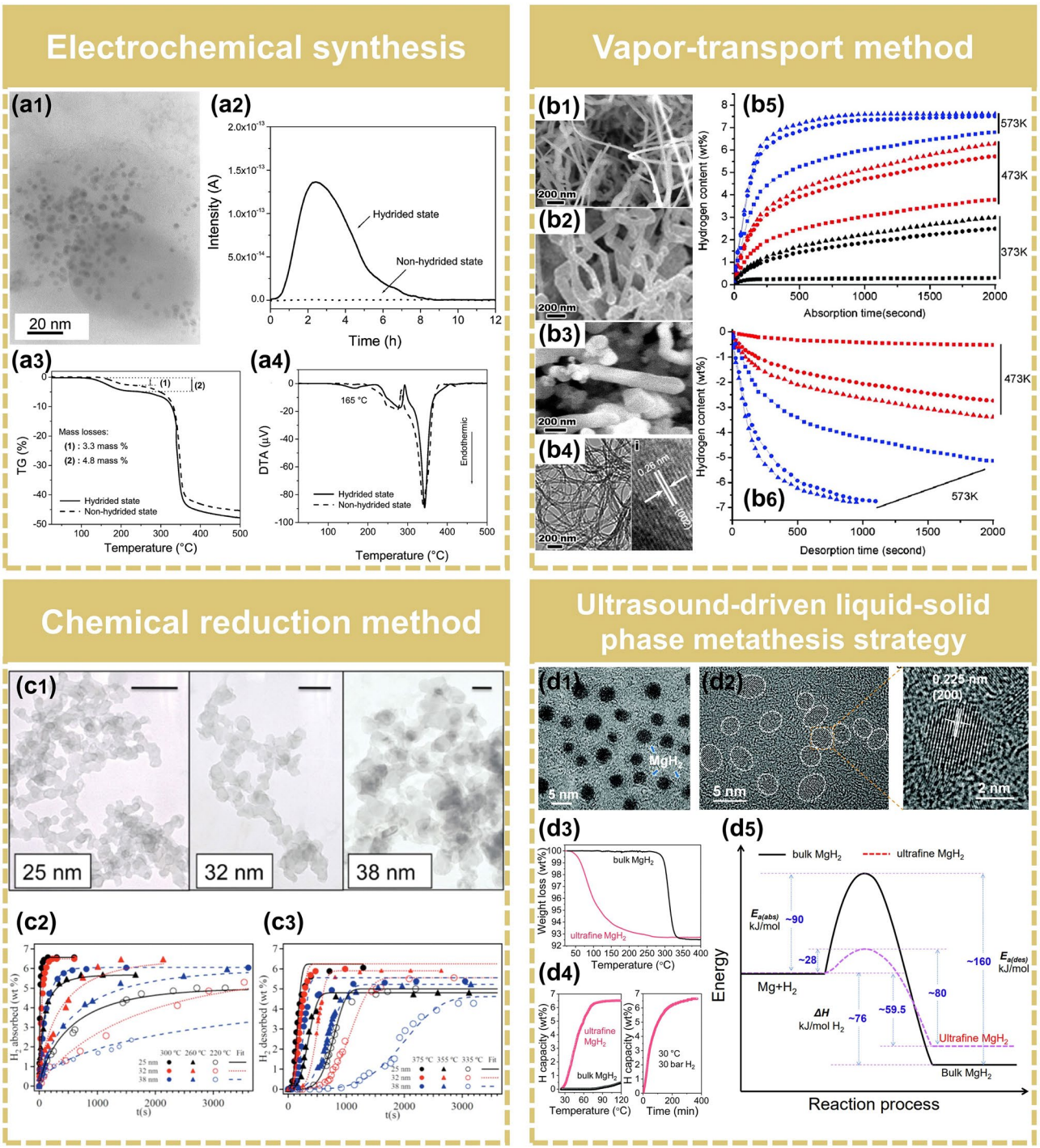

Fig. 4 Synthesis of the free-standing nano-sized Mg/MgH_2. **a1** TEM image of the Mg colloid synthesized by electrochemical method. **a2** Mass spectrometry of H_2 desorption for the MgH_2 (hydrided state) and the Mg colloids (non-hydrided state) at 85 °C. **a3**, **a4** TG-DSC signals of the Mg colloid after H_2 absorption (hydrided sate) and desorption (non-hydrided state). Reproduced with permission from Ref. [75]. Copyright 2008 American Chemical Society; **b1**–**b3** SEM images of Mg nanowires with a diameter of 30–50 nm, 80–100 nm and 150–170 nm, respectively. **b4** TEM and HRTEM images of Mg nanowires with a diameter of 30–50 nm. **b5** Hydrogen absorption and **b6** desorption curves of the Mg nanowires with different diameters (30–50 nm, triangle; 80–100 nm, circle; 150–170 nm, square). Reproduced with permission from Ref. [77]. Copyright 2007 American Chemical Society; **c1** TEM images of Mg nanocrystal samples (scale bar = 100 nm). **c2** Hydrogen absorption and **c3** desorption curves of the Mg nanocrystal samples at different temperatures. Reproduced with permission from Ref. [44]. Copyright 2011 American Chemical Society; **d1** TEM image and **d2** HRTEM images of non-confined ultrafine MgH_2. **d3** TGA curves of bulk MgH_2 and non-confined ultrafine MgH_2. **d4** Hydrogenation profile with temperature of bulk MgH_2 and non-confined ultrafine MgH_2, and isothermal hydrogenation curves of non-confined ultrafine MgH_2. **d5** Comparison of the energy barriers for the hydrogen absorption and desorption of bulk MgH_2 and non-confined ultrafine MgH_2. Reproduced with permission from Ref. [78]. Copyright 2021 Royal Society of Chemistry

 https://doi.org/10.1007/s40820-023-01041-5

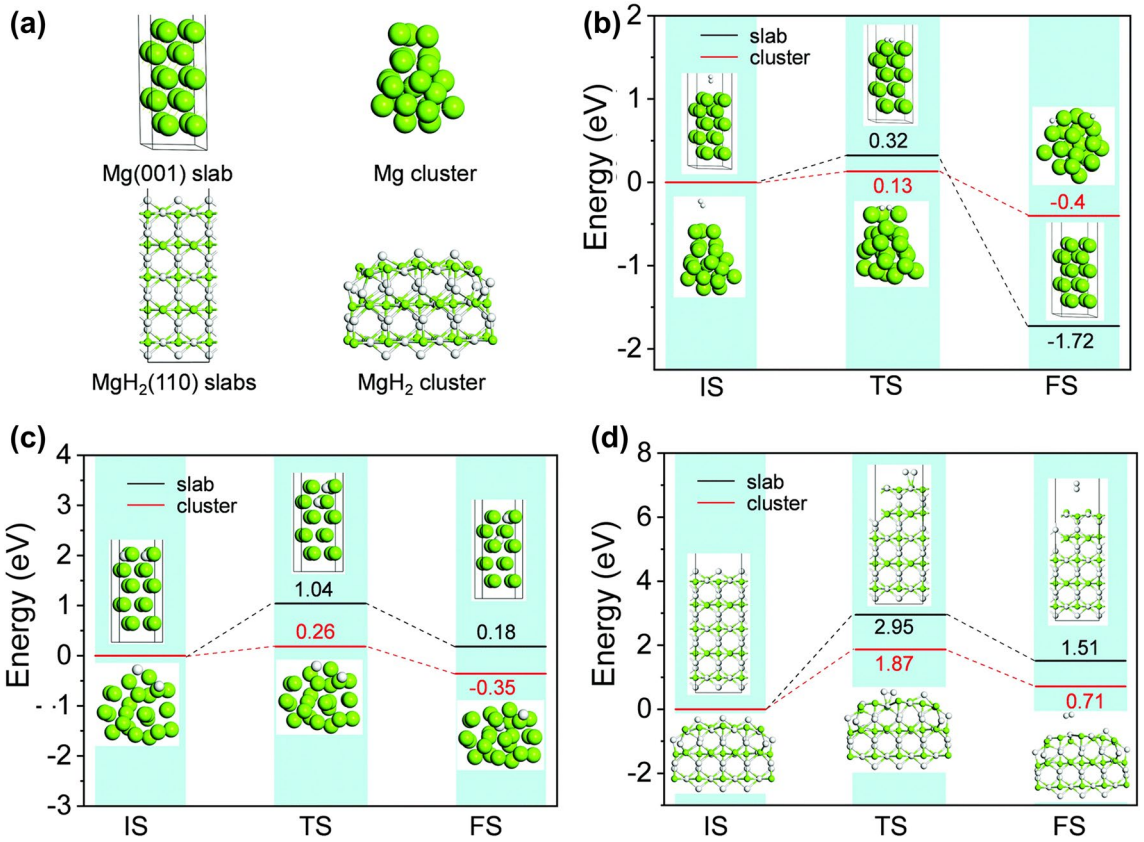

Fig. 5 **a** Computational structure models for bulk and nanosized Mg and MgH_2. **b** Hydrogen uptake by Mg (001) slab and Mg cluster. **c** Diffusion energy barrier of H atoms in the Mg (001) slab and Mg cluster. **d** Hydrogen release from MgH_2 (110) slab and MgH_2 cluster. Reproduced with permission from Ref. [78]. Copyright 2021 Royal Society of Chemistry. (IS: initial state, TS: transition state, FS: final state. Mg: green. H: white). (Colour figure online)

ball-milling method. Impressively, plentiful defects and nanocrystalline are ingeniously generated during the process of high-energy ball milling. The introduction of defects and reduction of particle size could provide more active sites for de/re-hydrogenation and shorten hydrogen diffusion paths, thereby improving the hydrogen ab/de-sorption kinetics.

As early as the late 1990s, Huot et al. [79] first prepared MgH_2 nanocrystals by using ball milling method. They found that the specific surface area of MgH_2 increased from 1.2 to 9.9 $m^2\ g^{-1}$ after ball milling, due to the reduction of particle size. However, the simple ball milling showed no obvious improvement in the performances of MgH_2. Usually, de/re-hydrogenation of MgH_2 is a catalytic reaction process depending on the catalytic activity of catalysts. Therefore, most of the research is focused on the introduction of catalysts into MgH_2 to fabricate nanostructured Mg-based composites via the ball-milling method. The combination of the disordered MgH_2 structure induced by mechanical milling with catalysts gives rise to synergetic effects and excellent ab/de-sorption properties.

Numerous catalysts can be introduced into MgH_2 system, including transition metals [33, 34, 70, 80, 81, 82, 83, 84], oxides [85, 86, 87, 88], carbides [89, 90, 91, 92, 93], nitrides [85, 94, 95], and halides [96]. These materials share some similarities. First, the 3d-metal additives could obviously reduce the activation energy of hydrogen desorption. Second, the transition metal catalysts could chemisorb hydrogen and accelerate the diffusion of hydrogen to the Mg matrix. Third, the interfaces created by the introduction of the catalysts could act as active nucleation sites for the hydride phase, which would reduce the nucleation barrier for MgH_2. Due to the above-mentioned similarities, the formation of

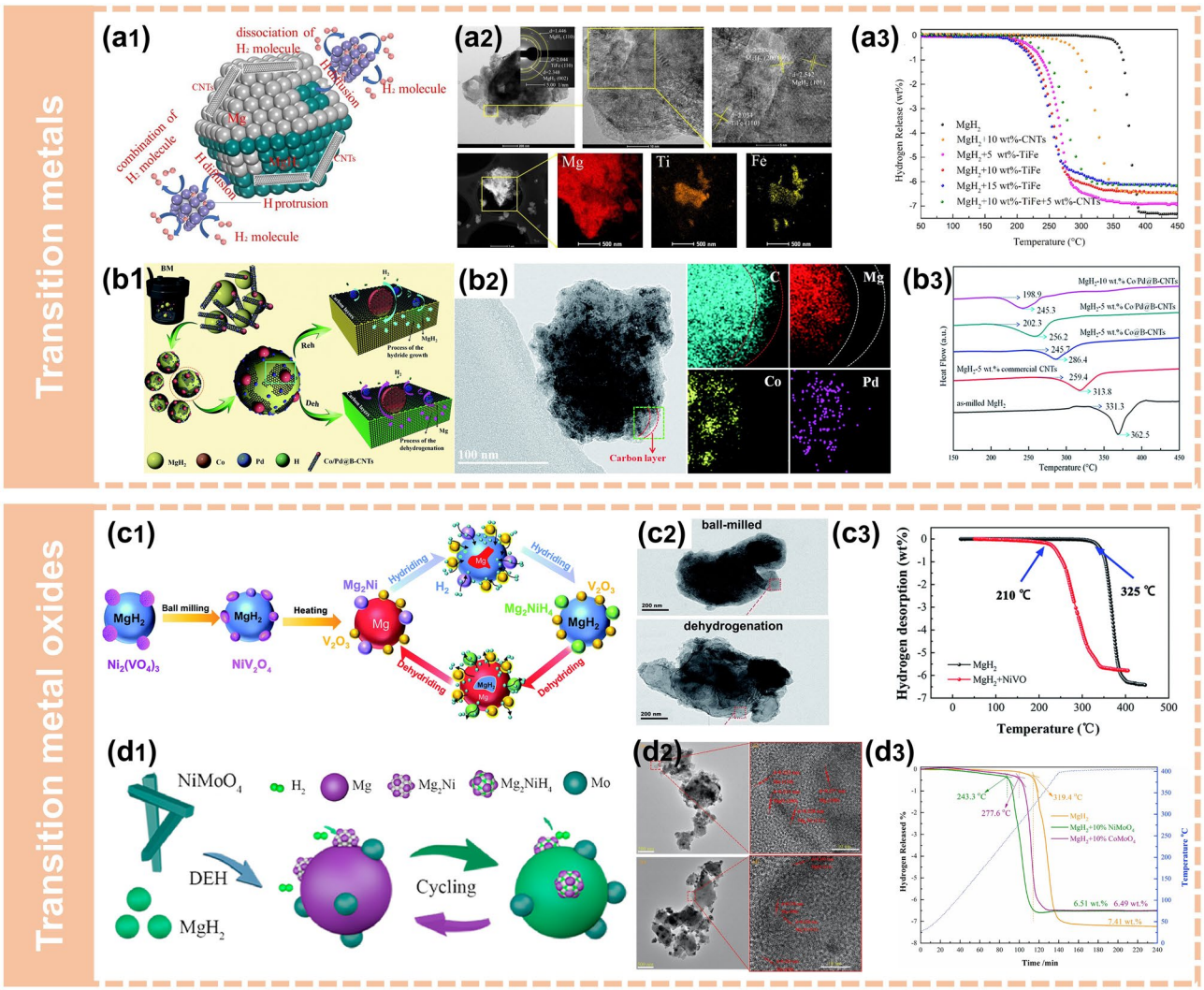

Fig. 6 Synthesis of nanostructured Mg-based composites via mechanical milling. **a1** Schematic summary of the catalytic mechanism for the TiFe and CNTs catalyzed MgH_2 particles. **a2** TEM images with corresponding SAED pattern and EDS mappings of the $MgH_2 + 10$ wt%-TiFe composite. **a3** Non-isothermal desorption curves of different samples. Reproduced with permission from Ref. [84]. Copyright 2021 Elsevier; **b1** A schematic illustration of the "bidirectional catalysis" mechanism of Co/Pd@B-CNTs during the dehydrogenation and hydrogenation of MgH_2. **b2** TEM images and EDS profiles of MgH_2–10 wt% Co/Pd@B-CNTs after ten cycles. **b3** DSC curves of different samples. Reproduced with permission from Ref. [97]. Copyright 2019 Royal Society of Chemistry; **c1** Schematic diagram of hydrogen absorption and desorption process. **c2** TEM images. **c3** TPD curves. Reproduced with permission from Ref. [98]. Copyright 2021 Royal Society of Chemistry; **d1** A schematic illustration of the dehydrogenation and hydrogenation process of the MgH_2–$NiMoO_4$ system. **d2** TEM and HRTEM images of MgH_2–10 wt% NiMoO4 after the 1st (top) and 10th (down) dehydrogenation. **d3** TPD curves. Reproduced with permission from Ref. [99]. Copyright 2021 Elsevier

high-performance nanostructured Mg-based hydrogen storage composites during ball-milling is expected.

Liang et al. [80] proposed MgH_2–TM (TM = Ti, V, Mn, Fe, Ni) nanocomposite powders through intensive mechanical milling. They found that the MgH_2–Ti and MgH_2–V nanocomposites exhibited rapid desorption kinetics above 523 K and absorption kinetics at temperature as low as 302 K. Furthermore, it is worth mentioning that the mechanically milled MgH_2–Ni nanocomposite exhibited better absorption kinetics than that of Mg–Ni alloy, due to the smaller particle size and better distribution of Ni-catalyst.

https://doi.org/10.1007/s40820-023-01041-5

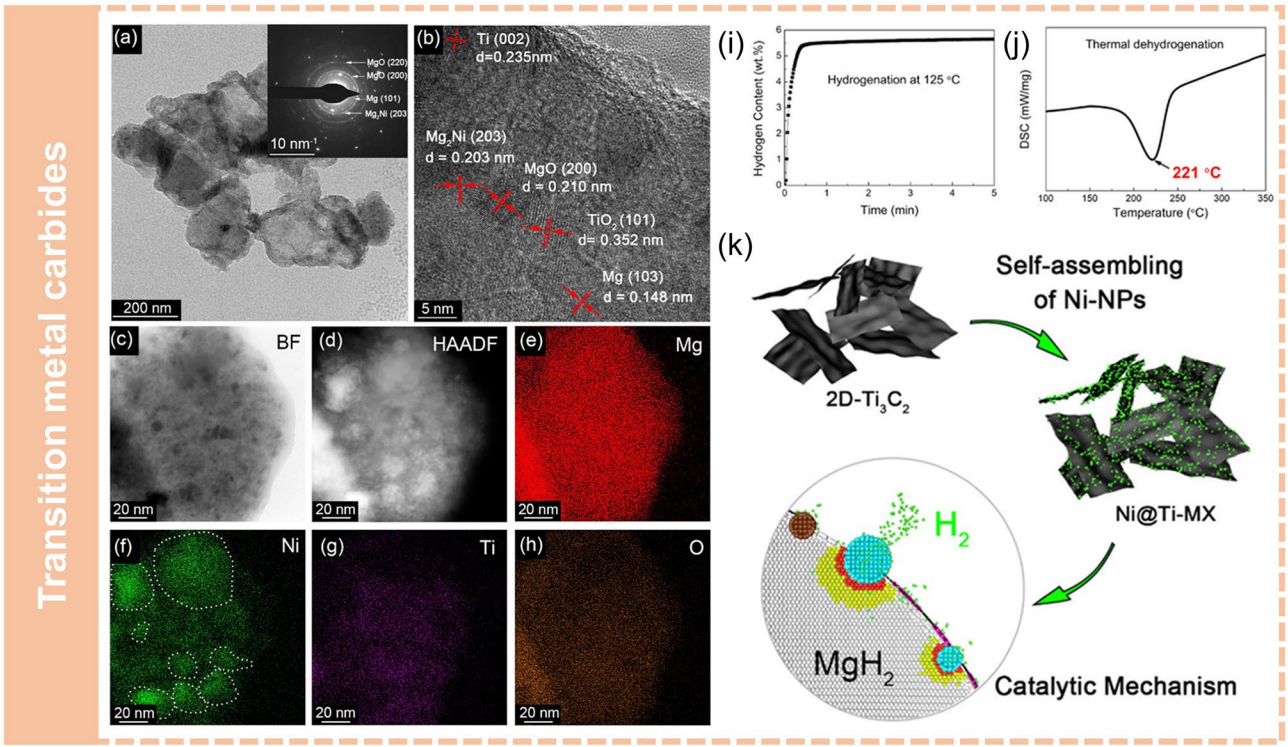

Fig. 7 Synthesis of nanostructured Mg-based composites via mechanical milling. **a** BF-TEM image and the corresponding SAED pattern (inset). **b** HRTEM image, and **c–h** EDS mapping of the dehydrogenated MgH_2 + Ni@Ti-MX composite. **i** Isothermal absorption curve of MgH_2 + Ni@Ti-MX at 125 °C. **j** DSC profiles of MgH_2 + Ni@Ti-MX at a heating rate of 3 °C min^{-1}. **k** Schematic illustrations of the synthesis process of Ni@Ti-MX and the proposed mechanism for fast hydrogen ab/de-sorption of MgH_2 + Ni@Ti-MX system. Reproduced with permission from Ref. [102]. Copyright 2020 American Chemical Society

Doping of nano-sized catalysts is crucial for enhancing the hydrogen storage performance of MgH_2, but it is less satisfactory to develop a single catalyst to enhance both hydrogen desorption and absorption properties to a certain degree. Therefore, the combination of two or more metal catalysts could further achieve simultaneous modification of the hydrogen absorption and release kinetics of MgH_2 [84, 97] (Fig. 6a, b). Liu et al. [97] introduced a bidirectional Co/Pd@B-CNTs into MgH_2 through ball milling (Fig. 6b1, b2). As depicted in Fig. 6b3, the composites presented superior hydrogen desorption properties at relatively low temperatures. They proposed a special mechanism for "bidirectional catalyst" Co/Pd, in which Pd accelerated the diffusion of hydrogen during the absorption process and phase transformation between Mg_2Co and Mg_2CoH_5 facilitated the release of hydrogen atoms.

Notably, the bimetallic oxides (e.g., $Ni_3(VO_4)_2$ [98], $TiNb_2O_7$ [100], Ni/$CoMoO_4$ [99]) have also been synthesized and applied to catalyze the re/de-hydrogenation of MgH_2 via mechanical milling (Fig. 6c, d). The introduction of multi-element metallic catalysts into MgH_2 by ball milling can not only make use of the synergistic effect from different metallic catalysts to enhance the hydrogen absorption and desorption performances of MgH_2 at the same time, but also effectively promote the uniform distribution of multiphase catalysts. Huang et al. [99] investigated the influence of the bimetallic oxides $NiMoO_4$ on the hydrogen storage properties of the MgH_2 (Fig. 6d). They demonstrated that "Mg_2Ni/Mg_2NiH_4" formed during hydrogen release/uptake process acted as "hydrogen pump" to boost the hydrogen storage performance of MgH_2. In situ formed Mo^0 not only weakened Mg–H bonding, but also further facilitated the mutual "Mg_2Ni/Mg_2NiH_4" transformation (Fig. 6d1, d2). Ascribing to the collaborative action between Ni– and Mo– containing species, the hydrogen storage kinetics of MgH_2 had been accelerated (Fig. 6d3).

To avoid growth and agglomeration of catalysts during re/de-hydrogenation at high temperatures, carbon-based

materials are used to load catalysts to promote their dispersion. For example, amorphous carbon-embedded porous Nb_2O_5 [101], $Ti_3C_2T_x$ supported Ni@C nanoflakes [89, 102, 103], carbon nanotube loaded multi-valence Co [34, 104], carbon-encapsulated ZrO_2 [36] etc. were successfully synthesized and milled with MgH_2 to improve hydrogen storage performances. It is worth emphasizing that the catalytic activity of catalysts loaded on carbon-based materials is much better than that of pure catalysts, due to the reduction of particle size, uniform distribution, and improvement of electrical conductivity.

Zhu et al. [102] synthesized a novel Ti_3C_2 MXene-based catalyst (Ni@Ti-MX) where ultra-dispersed Ni nanoparticles were anchored on the monolayer Ti_3C_2 flakes, and introduced into MgH_2 through ball milling to fabricate MgH_2 + Ni@Ti-MX nanocomposites (Fig. 7). Benefiting from the reduction of particle size during the ball milling process, the uniform dispersion of catalyst and the formation of multi-phase catalysts, the composites showed excellent performance. Hydrogen absorption at room temperature with a hydrogen storage capacity of 4 wt% was achieved. Particularly, the composites could absorb 5.4 wt% H_2 in 25 s at 125 °C and the desorption peak temperature reduced to 221 °C (Fig. 7i, j).

It is no doubt that the fabrication of nanostructured Mg-based hydrogen storage composites by ball-milling is an efficient and simple method to improve the kinetics of MgH_2. However, the nanoparticles generated by this method are typically large with an inhomogeneous size distribution, and extra impurities will be introduced. Moreover, the particles inevitably occur growth and self-aggregation during hydrogen cycling, resulting in hydrogen capacity decay. More importantly, the thermodynamics of Mg-based hydrogen storage composites prepared by ball-milling usually show no significant change, thus the desorption temperature of MgH_2 cannot be lowered below that of the bulk (573 K). On the basis of this, a novel material synthesis method, namely dielectric barrier discharge plasma-assisted milling (P-milling) was developed by Ouyang et al. [105, 106], which realized the dual tuning of the thermodynamic and kinetic properties of MgH_2. They reported that Mg(In)–MgF_2 composite synthesized by P-milling technique exhibited a much higher decomposition equilibrium than pure MgH_2 at the same temperature, which was caused by the rapid formation of a Mg-based solid solution [such as Mg(In)], confirming the thermodynamic destabilization. Meanwhile, the kinetics is also modified by the catalyzing effect of in situ formed MgF_2 during P-milling process, thus the dual tuning of thermodynamic and kinetic properties is realized.

3.3 Construction of Core–Shell Nanostructured Mg-Based Composites Through Chemical Reduction

Core–shell structures are of particular interest in the development of advanced composites as they can efficiently bring different components together at nanoscale. It has been widely employed in various fields including catalysis, energy, biology, and sensing. The advantage of this structure is greatly dependent on the distinctive synergistic effect between core and shell, thus obtaining a high-performance material.

Decoration of Mg nanoparticles with transition metal shells has become a widely used strategy to fabricate advanced nanostructured Mg-based hydrogen storage composites (Mg@TM) possessing potential advantages of encapsulation and catalysis effect originating from transition metal shells. The fabrication of Mg@TM core–shell structure could increase the contact area between the catalyst and hydrogen/matrix and provide more nucleation sites for MgH_2/Mg, making full use of catalytic activity of the catalyst and improving hydrogen storage performance of MgH_2. In addition, the strategy is simple, low-cost, and easy to scale up.

As a successful example, Cui et al. [107, 108] reported the fabrication of a series of unique Mg–TM core–shell structures through a facile chemical reaction of the pre-milled Mg powder with the corresponding chlorides. They found that the composition of the shell can be modulated from Ti to Nb, V, Co, Mo, and Ni by simply changing the cation of the precursor ($TiCl_3$, $NbCl_5$, VCl_3, $CoCl_2$, $MoCl_3$, $NiCl_2$) (Fig. 8a). During the process of chemical reduction, a portion of Mg reacted with the $TMCl_x$ to form a thin TM shell coating on the Mg core. This was completely different from the point contact of Mg/MgH_2 with the TM-based catalyst by ball-milling (Fig. 8a1). The results showed that composites can desorb hydrogen even under 200 °C (Fig. 8a2). Particularly, the dehydrogenation performance was in the

 https://doi.org/10.1007/s40820-023-01041-5

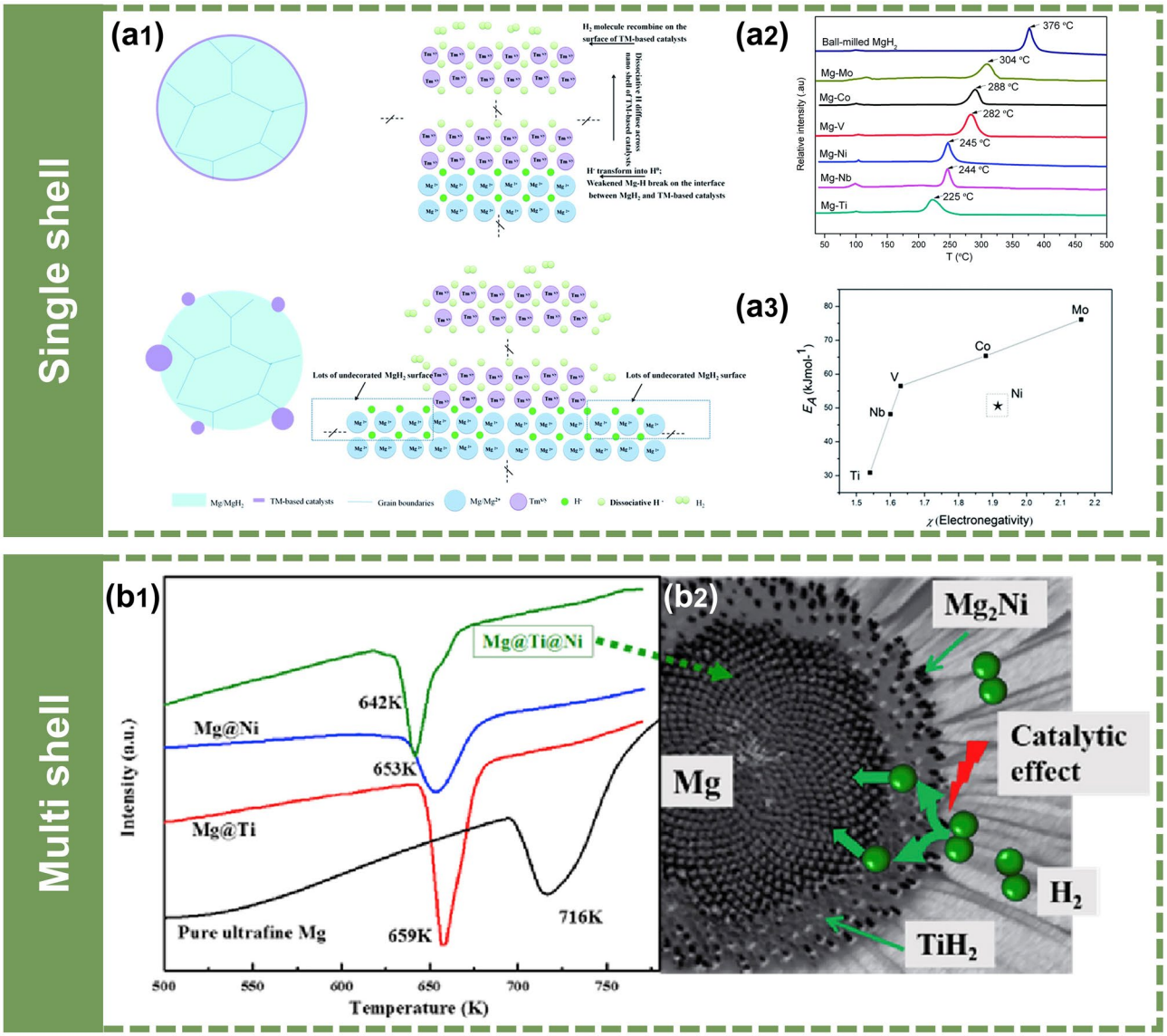

Fig. 8 Synthesis of core–shell nanostructured Mg-based composites through chemical reduction. **a1** A schematic diagram of the Mg–TM and ball-milled Mg–TM-based catalysts. **a2** TPD-MS curves of Mg–TM samples with a heating rate of 4 K min^{-1}. **a3** Plot of E_A verses χ of TM in Mg–TM systems. Reproduced with permission from Ref. [107]. Copyright 2014 Royal Society of Chemistry; **b1** DSC curves of different samples. **b2** A schematic diagram of Mg@Ti@Ni composite with core–shell structure. Reproduced with permission from Ref. [109]. Copyright 2017 Elsevier

sequence of Mg–Ti, Mg–Nb, Mg–Ni, Mg–V, Mg–Co, and Mg–Mo, due to the decrease in electro-negativity from Ti to Mo (Fig. 8a3).

As another example, Lu et al. [110] first synthesized a core–shell nanostructured Mg@Pt composite, consisting Mg particles as the core with nano-sized noble metal Pt particles distributed homogeneously on Mg ultrafine particles. According to the in-situ TEM observations and DFT calculation, they creatively demonstrated a new mechanism that the H-stabilized Mg_3Pt/Pt acted as the "hydrogen pump" for the dehydrogenation of MgH_2 to improve the dehydriding kinetics of the hydrogenated Mg@Pt composite, attributed to the unique core–shell structure of Mg@Pt.

Lu et al. [109] extended the chemical reduction strategy for the fabrication of multi-shelled ternary Mg@Ti@Ni composites (Fig. 8b). The synthesis process of Mg@Ti@

Ni core–shell structure included two-step electroless plating, namely, Cp_2TiCl_2 and $NiCl_2$ *n*-butyl were added to THF solution of Mg powder in sequence. According to the chemical reactions, they successfully prepared a ternary Mg@Ti@Ni core–shell structure. Attributing to the co-effect of TiH_2 acting as the activation site and Mg_2Ni acting as the "hydrogen pump", the composites exhibited excellent thermodynamic performance and accelerated hydrogenation kinetics.

3.4 Fabrication of Multi-dimensional Nano-sized Mg-Based Heterostructure Through Nanoconfinement Method

The nano-confinement method has been widely employed in the preparation of stabilized nanoparticles in the fields of energy storage and conversation. Recently, nano-confinement has been further proven to be an efficient process in constructing nanostructured Mg-based hydrogen storage composites.

Nano-confinement is the process in which a stable scaffold is acted as the substrate to support/confine nanoparticles/nanoclusters, inhibiting the growth and self-aggregation of the host [42, 43, 111]. The common features of these support materials are that they all possess high specific surface area and abundant porosity, providing sufficient nucleation sites for Mg/MgH_2. As a result, the growth and self-aggregation of nano-sized particles are conspicuously avoided, keeping an excellent nano-sized effect (such as more exposed active sites, high specific surface area, and shortened diffusion pathway) and ensuring stable and excellent hydrogen storage performances. Melt impregnation and liquid impregnation are two commonly used methods to achieve nanoconfinement of MgH_2/Mg.

The Mg precursor most widely used for the infiltration procedure is di-*n*-butyl-magnesium ($MgBu_2$) or bis-cyclopentadienyl magnesium ($MgCp_2$) [112], and then they were converted to MgH_2/Mg under hydrogen/argon atmosphere at high temperatures based on the following reactions:

$$MgBu_2 + H_2 \rightarrow MgH_2 + C_4H_{10} \quad (3\text{-}2)$$

$$MgCp_2 \rightarrow Mg + C_5H_5 \quad (3\text{-}3)$$

According to different operating conditions, the hydrogenation method of $MgBu_2$ can be divided into solid-state hydrogenation and liquid-state hydrogenation. The former refers that the hydrogenation process is performed after the solvent was completely evaporated. The procedure is described as follows: scaffolds are dispersed in $MgBu_2$ solution in Ar filled glove box; when the solvent (heptane) is completely evaporated, $MgBu_2$ is loaded onto the scaffolds; then the dried composites are transferred to the PCT reactor for further hydrogenation under the condition of 45 bar hydrogen pressure at 200 °C for 12 h. In terms of the liquid-state hydrogenation process, $MgBu_2$ is converted to MgH_2 through a solvothermal strategy under hydrogen atmosphere, and then solvent is completely evaporated to obtain MgH_2@scaffolds nanocomposites.

As early as 2005, Liang et al. [113] first suggested that the hydrogen desorption enthalpy for MgH_2 confined in carbon nanotube may be lowered and such confinement effect is independent of the tube length by theoretical calculations. Jongh et al. [114] successfully prepared Mg nano-crystallites by infiltration of nano-porous carbon with molten magnesium. Surprisingly, the Mg nanoparticles with a size smaller than 5 nm were first synthesized, which was never achieved before by unsupported nano-sized Mg/MgH_2. This is the first experimental study about the influence of both nanosizing and support interaction on hydrogen sorption properties of MgH_2.

To prevent excess $MgBu_2$ from sticking on the surface of the scaffold material, a multistep impregnation approach was developed for the fabrication of nano-confined Mg/MgH_2 [30, 115]. Zhao-Karger et al. [30] synthesized MgH_2 particles smaller than 3 nm confined in a carbon scaffold by repeating the procedures of impregnation/drying with 1.5 mL of $MgBu_2$ solution for each step along with the subsequent hydrogenation of $MgBu_2$. Liu et al. [115] first used the novel 1D bamboo-shaped carbon nanotubes (BCNTs) as carriers for the self-assembly of MgH_2 nanoparticles (15–20 nm) via repeating the procedures of impregnation/drying/hydrogenation three times (Fig. 9a). As a result, the extremely high loading capacity (76.8 mass fraction) was achieved and the obtained MgH_2@BCNTs showed remarkably improved thermodynamics and kinetics for H_2 adsorption and desorption.

It should be pointed out that, in a broad sense, if we define the shell structure composed of transition metal in core–shell nanostructured Mg@TM as an "encapsulation layer", construction of core–shell structure through chemical reduction can be regarded as a confinement approach as well. The only difference is that the encapsulation layer, which

 https://doi.org/10.1007/s40820-023-01041-5

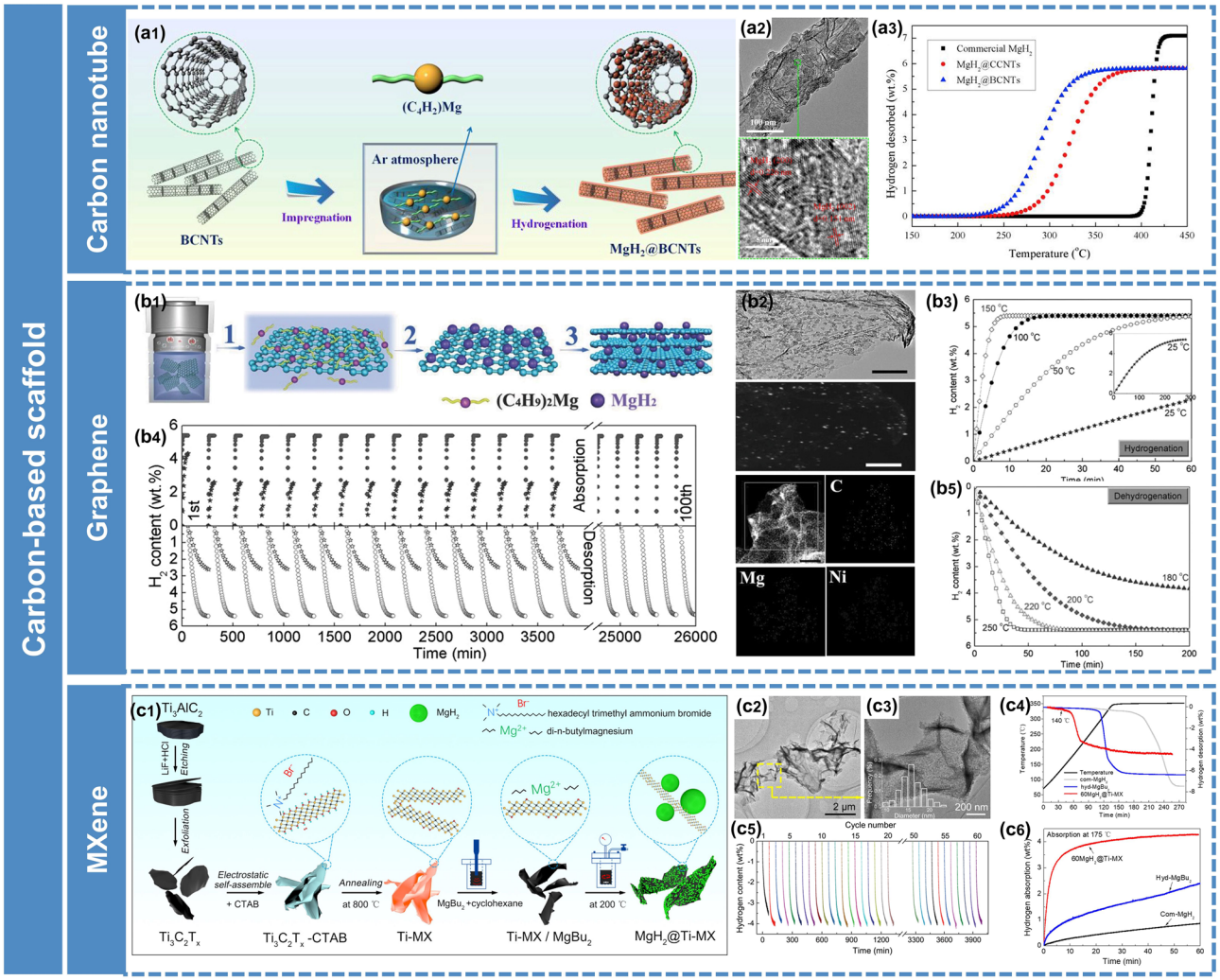

Fig. 9 Synthesis of nanostructured Mg-based composites through the nano-confinement method. **a1** Schematic illustration of the self-assembly of MgH_2 NPs on the BCNTs. **a2** Representative TEM and HRTEM images of MgH_2@BCNTs. **a3** TPD curves of different samples. Reproduced with permission from Ref. [115]. Copyright 2019 Elsevier. **b1** Schematic illustration of the self-assembly of MgH_2 NPs on GR. **b2** TEM, STEM images of Ni-MHGH-75, and corresponding elemental mapping images. **b3** Hydrogenation and **b5** dehydrogenation of Ni-MHGH-75 at various temperatures. **b4** Reversible H_2 absorption and desorption of Ni-MHGH-75 (circles) and MHGH-75 (stars) at 200 °C. Reproduced with permission from Ref. [116]. Copyright 2015 John Wiley and Sons; **c1** Schematic illustration of the fabrication of MgH_2@Ti-MX. **c2, c3** TEM images of the 60MgH_2@Ti-MX. **c4** TPD curves of different samples. **c5** Cycling dehydrogenation curves of 60MgH_2@Ti-MX at 200 °C. **c6** Isothermal hydrogenation curves of different samples. Reproduced with permission from Ref. [117]. Copyright 2021 American Chemical Society

can also prevent Mg/MgH_2 nanoparticles from growing up and agglomerating, is introduced later for the synthesis of core–shell structure.

Carbon-based materials have long been expected as promising supports for constructing nano-sized hydrogen storage materials, due to their excellent stability and high specific surface area. Xia et al. [116] reported that monodispersed MgH_2 nanoparticles were assembled on the graphene decorated with Ni, exhibiting remarkable hydrogen storage properties (Fig. 9b). However, graphene is susceptible to the interlaminar stacking due to the high π–π bonding energy and the strong physical cross-linking. Moreover, due to the inert surface of pure carbon materials, premodification is needed before confining metal hydrides, which is complex and may introduce pollutants or even impair the mechanical properties of carbon-based materials.

With the preceding understanding of the scaffold of nanoconfinement, intuitively, the novel materials, such as

MXenes, MOF, and transition metal compounds, which possess high specific surface area and intrinsic catalytic activity, could also act as superior scaffolds to support MgH_2 nanoparticles. Hence, our group used Ti_3C_2, Ni–MOF, MOF derivatives, TiO_2 nanosheets, etc. to fabricate the multi-dimensional Mg-based heterostructure to address the inert deficiency of pure carbon materials.

As promising 2D materials, MXenes have been widely investigated due to their special layered structure, excellent catalytic activity, high conductivity, and good flexibility [118, 119]. Numerous studies have focused on the introduction of MXenes as simple catalysts into MgH_2 through mechanical milling to improve kinetic properties [120]. However, simple ball-milling leads to the serious destruction of two-dimensional structure of MXenes, and their unique structural advantages cannot be fully exploited. By making full use of the structural advantages of MXenes, Zhu et al. [117] ingeniously designed 3D $Ti_3C_2T_x$ composed of folded $Ti_3C_2T_x$ nanosheets, and then used it as a scaffold to disperse MgH_2 nanoparticles to construct MgH_2@Ti-MX nanocomposites through a solvothermal strategy (Fig. 9c). The obtained composites exhibited excellent hydrogen ab/desorption kinetics and low hydrogen desorption temperature (T_{onset} = 140 °C), remarkably superior to that of the MgH_2 systems confined by pure carbon-based materials, attributed to the nano-size effect and the in situ formed catalytic TiH_2.

In addition to MXene, metal–organic frameworks (MOFs) based materials, including pristine MOFs, MOF composites, and their derivatives have attracted great attention as potential hydrogen storage materials. Due to their high specific surface area and unique porous structure, most of the researches on MOFs in the field of hydrogen storage have focused on physical adsorption. In 2012, a hybrid hydrogen storage material composed of MOF (SNU-90) and Mg nanocrystals was first reported, which could store H_2 by both physisorption and chemisorption [121].

The nano-confinement of MgH_2 in the mesoporous structure of a Ni-based metal–organic-framework (denoted as MgH_2@Ni–MOF) was also successfully conducted with $MgBu_2$ as precursor via a combination of solvothermal method and wet impregnation method followed by hydrogenation [125]. The results showed that MgH_2@Ni–MOF nanocomposites possessed rapid kinetic properties and low hydrogen ab/de-sorption enthalpy, which was attributed to the synergistic nano-size effect of nanoconfined Mg/MgH_2 in Ni–MOF and catalytic effects from in situ formed Mg_2Ni/Mg_2NiH_4. Notably, this is the first attempt that scaffold itself not only acts as an "aggregation blocker" to impede the growth and agglomeration of Mg/MgH_2, but also has excellent catalytic activity on the hydrogen sorption of MgH_2/Mg.

However, micropores of pristine MOFs always hinder the impregnation of $MgBu_2$ and the diffusion rate of H_2 through the pores, resulting in a low loading capacity of MgH_2 and limited improvement in performance. So far, huge attention and efforts have been paid to MOF derivatives [126]. Shinde et al. [122] presented a simple and scalable strategy to fabricate air-stable MgH_2 embedded in MOF-derived 3D activated carbon with periodic synchronization of transition metals (MHCH) (Fig. 10a). The resulting MHCH-5 (TM = Ni) exhibited excellent hydrogen storage properties, with a high storage capacity of 6.63 wt% H_2, rapid kinetics loading in < 5 min at 180 °C, superior reversibility, and excellent long-term cycling stability over ~ 435 h. They demonstrated that the synergetic effects of nanoconfinement, uniform distribution of MgH_2 NPs, exceptional structural and chemical stabilities, and high thermal conductivity contributed to the enhancement of hydrogen storage performance of MgH_2. In order to increase the load capacity of MgH_2 on the scaffold, Ma et al. [123] designed a novel CoS-nanoparticle-assembled nano boxes (denoted as CoS-NBs) scaffold derived from ZIF-67 with suitable mesoporous structure through a template-consumption method. And then MgH_2 was confined within the porous structure of CoS-NBs (referred to as MgH_2@CoS-NBs) by a wet impregnation method followed by hydrogenation at elevated temperatures (Fig. 10b). Benefiting from the appropriate mesoporous structure and excellent catalytic activity of CoS, the load capacity of MgH_2 was up to 42.5 wt% and the hydriding/dehydriding enthalpies reduced to − 65.6/68.1 kJ mol^{-1} H_2. Based on the structural designing strategies of MOFs, Zou et al. [127] further constructed a MOF-derived 1D *N*-doped hierarchically porous carbon nanofiber and used it as the scaffold for self-assembly of MgH_2/Ni nanoparticles.

Besides the scaffolds mentioned above, we have recently discovered that 2D transition metal oxides (TiO_2) nanosheets are also promising frameworks to host MgH_2 nanoparticles (Fig. 10c) [124]. The results demonstrated the significant contribution of the nanoconfinement effect and Mg–Ti

 https://doi.org/10.1007/s40820-023-01041-5

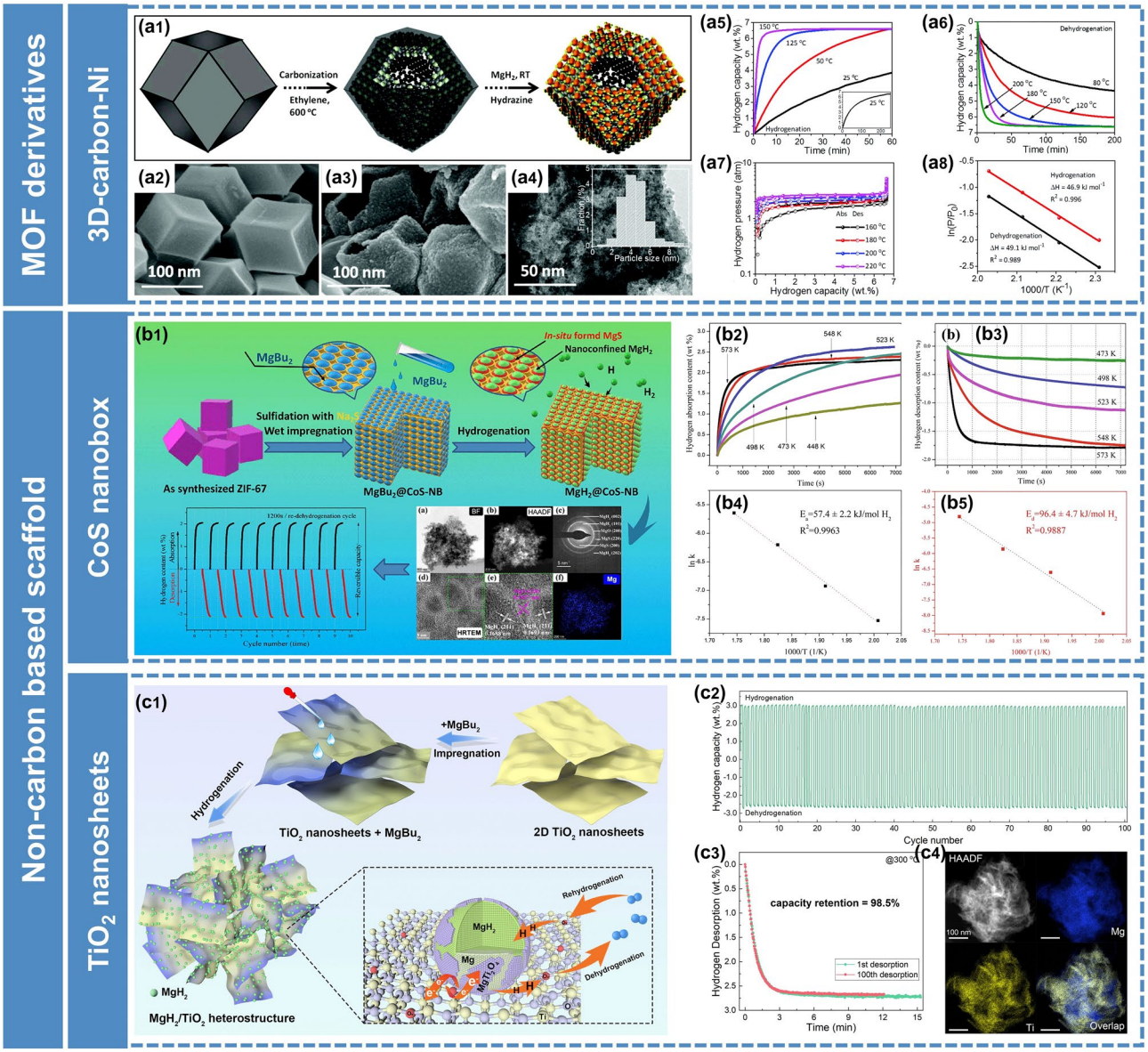

Fig. 10 Synthesis of nanostructured Mg-based composites through nano-confinement method. **a1** Schematics displaying the self-assembled MgH_2 on 3D metal interacted carbon. **a2** SEM image of the prepared metal-interacted 3-D carbon. **a3** SEM and **a4** TEM images of the MHCH-5. **a5** Hydrogen absorption and **a6** desorption of the MHCH-5 at different temperatures. **a7** Pressure–composition–temperature (PCT) plots of the MHCH-5 at different temperatures. **a8** The van't Hoff plots of the MHCH-5 derived from de-/hydrogenation. Reproduced with permission from Ref. [122]. Copyright 2017 Royal Society of Chemistry; **b1** Schematic illustrations of the nanoconfinement process for the synthesis of MgH_2@CoS-NBs composite, TEM images of MgH_2@CoS-NBs, and cycling behavior of the MgH_2@CoS-NBs composite. **b2** Isothermal hydriding and **b3** dehydriding profiles, and the corresponding *lnk* verses 1000/*T* plots for determining the activation energy of **b4** hydrogenation and **b5** dehydrogenation. Reproduced with permission from Ref. [123]. Copyright 2021 Elsevier; **c1** synthesis process of MgH_2/TiO_2 composites and schematic diagram showing the hydrogenation and dehydrogenation mechanisms of MgH_2/TiO_2 heterostructure. **c2** Cycling profiles of $60MgH_2/TiO_2$ at 300 °C. **c3** Hydrogen desorption curves of $60MgH_2/TiO_2$ at different cycles. **c4** HAADF images of $60MgH_2/TiO_2$ after 100 cycles and corresponding EDS elemental mapping results. Reproduced with permission from Ref. [124]. Copyright 2022 Springer Nature

oxides to re/de-hydrogenation performances. It was worth emphasizing that abundant oxygen vacancies were introduced into TiO_2 nanosheets during the impregnation process due to the strong reducibility of $MgBu_2$, which had a positive influence on the improvement of MgH_2.

Based on the above review, we concluded that significant breakthroughs in nanostructured Mg-based hydrogen storage

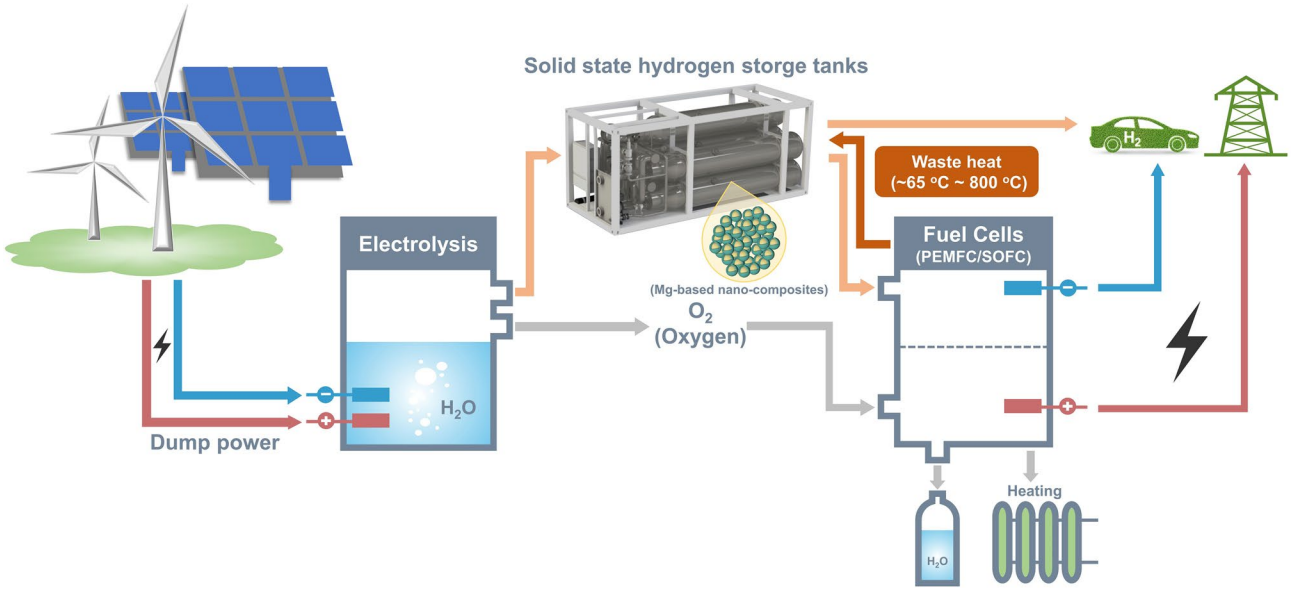

Fig. 11 A vision of the future energy infrastructure (electrolysis system; safety design for the hydrogen storage and transportation device; construction of hydrogen system-linked hydrogen vehicles/fuel cell equipment charging system)

materials were made in recent years, and their application for stationary/on-board hydrogen storage would be within sight.

4 Promising Applications of Nanostructured Mg-Based Hydrogens Storage Materials

We have a bright vision of the new energy structure of "renewable energy for hydrogen production—hydrogen storage—transportation integration" in the future (Fig. 11). Hydrogen can be produced by electrolysis of water using electricity generated from clean energy sources, and the hydrogen is stored in a Mg-based hydrogen storage tanks. This system could supply high-purity hydrogen gas to a fuel cell for electricity generation or other industry usage at the same time. In turn, waste heat generated by PEMFC/SOFC can be used to provide energy for continued hydrogen release from the hydrogen storage tanks.

Compared with $LaNi_5$-based materials and Ti–V(Cr)-based alloys with body-centered cubic structures, MgH_2 has the promising potential to satisfy technical requirements for both gravimetric and volumetric capacities. Moreover, considering the cost and energy density of MgH_2, it is very promising for small-scale portable applications to supply hydrogen through the hydrolysis reaction in water [128, 129]. Notably, nanostructured MgH_2/Mg will improve the performances of the hydrolysis reaction, making it more efficient and convenient for small-scale portable applications.

Furthermore, MgH_2 has the advantages of large heat storage density (3060 kJ kg^{-1}), excellent reversibility, and low cost, which is available for large-scale heat storage to store excess heat from solar power plants or industries [130]. This is one of the hot research topics in chemical heat storage. In the daytime, excess solar energy can be used to promote the decomposition of MgH_2, and the hydrogen can be stored in the hydrogen tank or low-temperature hydrogen-storage materials. At night, a heat energy density of 0.9 kWh kg_{Mg}^{-1} will be released through the hydrogen absorption in Mg. It is noteworthy that additional catalysts need to be introduced into the MgH_2/Mg system to improve its thermal storage efficiency; the cost of this part is difficult to estimate. If the synthesis process for the low-cost and large-scale nanosized Mg-based hydrogen storage materials can be developed, significant cost savings for thermal storage systems will be achieved through the use of nanostructured Mg-based hydrogen storage materials.

Impressively, nanostructured Mg/MgH_2 can also be used as reactant of integrated Li(Na)BH_4 hydrogen production/storage technology to maximize the regeneration efficiency of Li(Na)BH_4 [131, 132, 133], which is the new topic for hydrogen-energy chain and hydrogen economics. What's more, nanostructured Mg-based hydride has also been

 https://doi.org/10.1007/s40820-023-01041-5

successfully used as an advanced battery anode material for lithium-ion storage [134, 135, 136]. Indubitably, nanostructured Mg-based hydrogen storage materials will play a critical role in the future energy structure.

5 Conclusion and Outlook

Herein, we have highlighted the most important synthetic methodologies and hydrogen storage applications of nanostructured Mg-based composites. Significant advances have been made in the fabrication of nanostructured Mg-based hydrogen storage materials in the last decades, accompanied by several breakthroughs in hydrogen storage performances toward industrial applications. Especially, near room temperature reversible hydrogen ab/de-sorption (30 °C) with considerable high capacity (> 6.7 wt%) has been achieved. Additionally, dual regulation of nanoconfinement and nanocatalysis has been realized. Moreover, the low ab/de-sorption temperature achieved by modified MgH_2 has fallen into the range of proton exchange membrane (PEM) fuel cells, which is a big step forward for the application of nanostructured Mg-based hydrogen storage composites in the field of transportation. What's more, nanostructured Mg-based hydride has been successfully used as an advanced battery anode material for lithium-ion storage.

It is well known that all modifications of MgH_2 have the same goals, i.e., lower working temperature, higher hydrogen storage capacity, and better cycling stability with lower cost and easier production process. With our current knowledge, it is worth emphasizing that the improvement of the properties of MgH_2/Mg towards theoretical capacity of 7.6 mass% (110 g L^{-1}) below 100 °C and long-term cyclic stability depends upon the choice of appropriate synthetic approaches to enable the full control over both kinetics and thermodynamics. For future research in the synthesis and application of nanostructured Mg-based hydrogen storage composites, we believe that it should concentrate on the following aspects:

(a) Most of the conventional methodologies suffer from one or more of the following deficiencies: difficulty in precise control and lack of uniformity and universality. Typically, the thermodynamics will be modified first and then some catalysts will be added. Such an approach generally results in capacity loss and sometimes additional degradation of the hydrogen properties due to the lack of "compatibility" between the catalyst, the hydride, and the thermodynamic enhancer. Thus, new synthetic strategies need to be developed to achieve precise position control of alloying elements and catalysts in Mg/MgH_2 lattice at the atomic level to maximize their effects while retaining the hydrogen storage capacity of hydride.

(b) Nanoconfinement strategy has the disadvantage of troublesome synthesis procedure, unfeasible for mass production, and high cost. In this regard, the development of facile, versatile, low-cost, and scalable methods for the production of high-quality nanostructured Mg-based hydrogen storage materials and precisely controlled structural parameters is of primary importance. And the most notable point is that the commonly used precursor of $MgBu_2$ in the synthesis of nanoconfined MgH_2 nanoparticles, generally has disadvantages such as complex synthesis process, being expensive, and being prone to oxidation. Hence, in order to simplify the synthesis process of nanoconfined MgH_2/Mg with "clean" and hydrogen active surfaces, new Mg precursors with high safety, low cost, good solubility in common solvents, low decomposition temperatures, and/or low reduction potential should be synthesized and the design of effective organic stabilizer should be pursued.

(c) To date, most studies about the scaffold of nanoconfinement strategy have focused on stable carbon materials (such as carbon nanotube and graphene), while complex oxide and nitride frameworks have rarely been reported. Given their unique catalytic activity, the fabrication of oxide and nitride frameworks with high specific surface areas is of great importance. Moreover, a novel scaffold with nano-confinement capability for hydride, high catalytic activity, and physical hydrogen storage capacity is highly desired, so that unique nanostructured Mg-based hydrogen storage composites with high capacity and superior performances can be synthesized combining both physical and chemical hydrogen storage.

(d) Lots of nanostructured Mg-based hydrogen storage materials are prepared relying on the experiences of researchers. The rational design of Mg-based hydrogen storage materials for specific applications based on material genome engineering technology remains a great challenge and should be strengthened in the future.

(e) The catalytic mechanism of some catalysts for Mg-based hydrogen storage materials remains elusive. It would be very helpful to deepen the comprehension and understanding of the catalytic mechanism, espe-

cially from the atomic level, which would spur novel and powerful methodologies for the construction of high-performance Mg-based hydrogen storage materials.

(f) The new energy storage infrastructure of "renewable energy for hydrogen production—hydrogen storage—transportation integration" should be taken into account in the future. Moreover, effective thermal management is also critical to the application of nanostructured Mg-based hydrogen storage materials in the field of on-board hydrogen storage.

The breakthroughs in the construction of nanostructured Mg-based hydrogen storage composites have provided opportunities to tune their hydrogen storage properties. Although MgH_2 has been extensively studied as one of the most promising solid-state hydrogen storage materials, its application in other energy fields has attracted little attention. Considering the low cost and unique phase transformation behavior, we expect to see a surge in the application of nanostructured Mg-based hydrogen storage materials in various energy fields, such as energy storage of renewable energy.

Lastly, it should be emphasized that the kinetic and thermodynamic properties of nanostructured Mg-based hydrogen storage composites are still far from the requirements for the on-board applications. There is still a long way to go for the commercial-scale production and practical application of such intriguing materials. Although we have summarized some recent advances on the synthesis of nanostructured Mg-based hydrogen storage composites, we would rather regard this review as an opening remark than a concluding remark. We are confident that other versatile and powerful synthetic methodologies for nanostructured Mg-based composites will be developed in the future. We also believe that nanostructured Mg-based hydrogen storage materials will have a place in the fields of energy storage and conversion.

Acknowledgements Prof. Zou would like to thank the support from the National Key Research & Development Program (2022YFB3803700) of China and National Natural Science Foundation (No. 52171186). The authors also appreciate the financial support from the Center of Hydrogen Science, Shanghai Jiao Tong University.

Funding Open access funding provided by Shanghai Jiao Tong University.

References

1. G.W. Crabtree, M.S. Dresselhaus, The hydrogen fuel alternative. MRS Bull. **33**(4), 421–428 (2011). https://doi.org/10.1557/mrs2008.84
2. M. Dornheim, N. Eigen, G. Barkhordarian, T. Klassen, R. Bormann, Tailoring hydrogen storage materials towards application. Adv. Eng. Mater. **8**(5), 377–385 (2006). https://doi.org/10.1002/adem.200600018
3. J.O. Abe, A.P.I. Popoola, E. Ajenifuja, O.M. Popoola, Hydrogen energy, economy and storage: review and recommendation. Int. J. Hydrogen Energy **44**(29), 15072–15086 (2019). https://doi.org/10.1016/j.ijhydene.2019.04.068
4. L. Schlapbach, Hydrogen-fuelled vehicles. Nature **460**(7257), 809–811 (2009). https://doi.org/10.1038/460809a
5. Z. Abdin, A. Zafaranloo, A. Rafiee, W. Mérida, W. Lipiński et al., Hydrogen as an energy vector. Renew. Sustain. Energy Rev. **120**, 109620 (2020). https://doi.org/10.1016/j.rser.2019.109620
6. J. Yang, A. Sudik, C. Wolverton, D.J. Siegel, High capacity hydrogen storage materials: attributes for automotive applications and techniques for materials discovery. Chem. Soc. Rev. **39**(2), 656–675 (2010). https://doi.org/10.1039/B802882F
7. I. Staffell, D. Scamman, A. Velazquez Abad, P. Balcombe, P.E. Dodds et al., The role of hydrogen and fuel cells in the global energy system. Energy Environ. Sci. **12**(2), 463–491 (2019). https://doi.org/10.1039/C8EE01157E
8. M.G. Rasul, M.A. Hazrat, M.A. Sattar, M.I. Jahirul, M.J. Shearer, The future of hydrogen: challenges on production, storage and applications. Energy Convers. Manag. **272**, 116326 (2022). https://doi.org/10.1016/j.enconman.2022.116326
9. T. Capurso, M. Stefanizzi, M. Torresi, S.M. Camporeale, Perspective of the role of hydrogen in the 21st century energy transition. Energy Convers. Manag. **251**, 114898 (2022). https://doi.org/10.1016/j.enconman.2021.114898
10. M.R. Usman, Hydrogen storage methods: review and current status. Renew. Sustain. Energy Rev. **167**, 112743 (2022). https://doi.org/10.1016/j.rser.2022.112743
11. J. Zheng, X. Liu, P. Xu, P. Liu, Y. Zhao et al., Development of high pressure gaseous hydrogen storage technologies. Int.

J. Hydrogen Energy **37**(1), 1048–1057 (2012). https://doi.org/10.1016/j.ijhydene.2011.02.125

12. J. Zheng, L. Chen, J. Wang, X. Xi, H. Zhu et al., Thermodynamic analysis and comparison of four insulation schemes for liquid hydrogen storage tank. Energy Convers. Manag. **186**, 526–534 (2019). https://doi.org/10.1016/j.enconman.2019.02.073
13. Z. Chen, K.O. Kirlikovali, K.B. Idrees, M.C. Wasson, O.K. Farha, Porous materials for hydrogen storage. Chem **8**(3), 693–716 (2022). https://doi.org/10.1016/j.chempr.2022.01.012
14. L. Ouyang, K. Chen, J. Jiang, X.-S. Yang, M. Zhu, Hydrogen storage in light-metal based systems: a review. J. Alloys Compd. **829**, 154597 (2020). https://doi.org/10.1016/j.jallcom.2020.154597
15. B. Sakintuna, F. Lamari-Darkrim, M. Hirscher, Metal hydride materials for solid hydrogen storage: a review. Int. J. Hydrogen Energy **32**(9), 1121–1140 (2007). https://doi.org/10.1016/j.ijhydene.2006.11.022
16. C. Weidenthaler, M. Felderhoff, Solid-state hydrogen storage for mobile applications: Quo Vadis? Energy Environ. Sci. **4**(7), 2495–2502 (2011). https://doi.org/10.1039/c0ee00771d
17. F. Cheng, Z. Tao, J. Liang, J. Chen, Efficient hydrogen storage with the combination of lightweight Mg/MgH_2 and nanostructures. Chem. Commun. **48**(59), 7334–7343 (2012). https://doi.org/10.1039/C2CC30740E
18. C. Zhou, Y. Peng, Q. Zhang, Growth kinetics of MgH_2 nanocrystallites prepared by ball milling. J. Mater. Sci. Technol. **50**, 178–183 (2020). https://doi.org/10.1016/j.jmst.2020.01.063
19. S. Dong, C. Li, J. Wang, H. Liu, Z. Ding et al., The "burst effect" of hydrogen desorption in MgH_2 dehydrogenation. J. Mater. Chem. A **10**, 22363–22372 (2022). https://doi.org/10.1039/d2ta06458h
20. Y. Shang, C. Pistidda, G. Gizer, T. Klassen, M. Dornheim, Mg-based materials for hydrogen storage. J. Magnes. Alloys **9**(6), 1837–1860 (2021). https://doi.org/10.1016/j.jma.2021.06.007
21. P. Liu, J. Lian, H. Chen, X. Liu, Y. Chen et al., In-situ synthesis of Mg_2Ni–Ce_6O_{11} catalyst for improvement of hydrogen storage in magnesium. Chem. Eng. J. **385**, 123448 (2020). https://doi.org/10.1016/j.cej.2019.123448
22. X. Ding, R. Chen, X. Chen, H. Fang, Q. Wang et al., A novel method towards improving the hydrogen storage properties of hypoeutectic Mg–Ni alloy via ultrasonic treatment. J. Magnes. Alloys (2021). https://doi.org/10.1016/j.jma.2021.06.003
23. F. Guo, T. Zhang, L. Shi, L. Song, Hydrogen absorption/desorption cycling performance of Mg-based alloys with in-situ formed Mg_2Ni and LaH_x (x = 2, 3) nanocrystallines. J. Magnes. Alloys (2021). https://doi.org/10.1016/j.jma.2021.06.013
24. N. Terashita, K. Kobayashi, T. Sasai, E. Akiba, Structural and hydriding properties of $(Mg_{1-x}Ca_x)Ni_2$ Laves phase alloys. J. Alloys Compd. **327**(1), 275–280 (2001). https://doi.org/10.1016/S0925-8388(01)01563-8
25. N. Ding, Y. Li, F. Liang, B. Liu, W. Liu et al., Highly efficient hydrogen storage capacity of 2.5 wt% above 0.1 MPa using Y and Cr codoped V-based alloys. ACS Appl. Energy Mater. **5**(3), 3282–3289 (2022). https://doi.org/10.1021/acsaem.1c03901
26. J. Huot, G. Liang, R. Schulz, Mechanically alloyed metal hydride systems. Appl. Phys. A: Mater. Sci. Process. **72**(2), 187–195 (2001). https://doi.org/10.1007/s003390100772
27. Y. Sun, T. Ma, K.-F. Aguey-Zinsou, Magnesium supported on nickel nanobelts for hydrogen storage: coupling nanosizing and catalysis. ACS Appl. Nano Mater. **1**(3), 1272–1279 (2018). https://doi.org/10.1021/acsanm.8b00033
28. J. Zhang, Y. Zhu, H. Lin, Y. Liu, Y. Zhang et al., Metal hydride nanoparticles with ultrahigh structural stability and hydrogen storage activity derived from microencapsulated nanoconfinement. Adv. Mater. **29**(24), 1700760 (2017). https://doi.org/10.1002/adma.201700760
29. D. He, Y. Wang, C. Wu, Q. Li, W. Ding et al., Enhanced hydrogen desorption properties of magnesium hydride by coupling non-metal doping and nano-confinement. Appl. Phys. Lett. **10**(1063/1), 4938245 (2015)
30. Z. Zhao-Karger, J. Hu, A. Roth, D. Wang, C. Kübel et al., Altered thermodynamic and kinetic properties of MgH_2 infiltrated in microporous scaffold. Chem. Commun. **46**, 8353–8355 (2010). https://doi.org/10.1039/C0CC03072D
31. G. Xia, L. Zhang, X. Chen, Y. Huang, D. Sun et al., Carbon hollow nanobubbles on porous carbon nanofibers: an ideal host for high-performance sodium–sulfur batteries and hydrogen storage. Energy Storage Mater. **14**, 314–323 (2018). https://doi.org/10.1016/j.ensm.2018.05.008
32. M. Lotoskyy, R. Denys, V.A. Yartys, J. Eriksen, J. Goh et al., An outstanding effect of graphite in nano-MgH_2–TiH_2 on hydrogen storage performance. J. Mater. Chem. A **6**(23), 10740–10754 (2018). https://doi.org/10.1039/C8TA02969E
33. Z. Yuan, S. Li, K. Wang, N. Xu, W. Sun et al., In-situ formed Pt nano-clusters serving as destabilization-catalysis bi-functional additive for MgH_2. Chem. Eng. J. (2022). https://doi.org/10.1016/j.cej.2022.135050
34. B. Liu, B. Zhang, X. Chen, Y. Lv, H. Huang et al., Remarkable enhancement and electronic mechanism for hydrogen storage kinetics of Mg nano-composite by a multi-valence Co-based catalyst. Mater. Today Nano **17**, 100168 (2022). https://doi.org/10.1016/j.mtnano.2021.100168
35. C. Meng, P. Yanhui, L. Zhenyang, H. Gang, L. Xiaofang et al., Synergy between metallic components of MoNi alloy for catalyzing highly efficient hydrogen storage of MgH_2. Nano Res. **13**(8), 2063–2071 (2020). https://doi.org/10.1007/s12274-020-2808-7
36. M. Chen, X. Xiao, X. Wang, Y. Lu, M. Zhang et al., Self-templated carbon enhancing catalytic effect of ZrO_2 nanoparticles on the excellent dehydrogenation kinetics of MgH_2. Carbon **166**, 46–55 (2020). https://doi.org/10.1016/j.carbon.2020.05.025
37. J.J. Reilly, R.H. Wiswall, Reaction of hydrogen with alloys of magnesium and nickel and the formation of Mg_2NiH_4.

Inorg. Chem. **7**(11), 2254–2256 (1968). https://doi.org/10.1021/ic50069a016

38. S.V. Halilov, D.J. Singh, M. Gupta, R. Gupta, Stability and electronic structure of the complex K_2PtCl_6-structure hydrides DMH_6 (D = Mg, Ca, Sr; M = Fe, Ru, Os). Phys. Rev. B **70**(19), 195117 (2004). https://doi.org/10.1103/PhysRevB.70.195117
39. J. Harris, On the adsorption and desorption of H_2 at metal surfaces. Appl. Phys. A **47**(1), 63–71 (1988). https://doi.org/10.1007/BF00619699
40. X. Huang, X. Xiao, Y. He, Z. Yao, X. Ye, H. Kou, C. Chen, T. Huang, X. Fan, L. Chen, Probing an intermediate state by X-ray absorption near-edge structure in nickel-doped $2LiBH_4$–MgH_2 reactive hydride composite at moderate temperature. Mater. Today Nano **12**, 100090 (2020). https://doi.org/10.1016/j.mtnano.2020.100090
41. X. Wang, X. Xiao, Z. Liang, S. Zhang, J. Qi et al., Ultrahigh reversible hydrogen capacity and synergetic mechanism of $2LiBH_4$–MgH_2 system catalyzed by dual-metal fluoride. Chem. Eng. J. **433**, 134482 (2022). https://doi.org/10.1016/j.cej.2021.134482
42. M. Rueda, L.M. Sanz-Moral, Á. Martín, Innovative methods to enhance the properties of solid hydrogen storage materials based on hydrides through nanoconfinement: a review. J. Supercrit. Fluids **141**, 198–217 (2018). https://doi.org/10.1016/j.supflu.2018.02.010
43. X.L. Zhang, Y.F. Liu, X. Zhang, J.J. Hu, M.X. Gao et al., Empowering hydrogen storage performance of MgH_2 by nanoengineering and nanocatalysis. Mater. Today Nano **9**, 100064 (2020). https://doi.org/10.1016/j.mtnano.2019.100064
44. N.S. Norberg, T.S. Arthur, S.J. Fredrick, A.L. Prieto, Size-dependent hydrogen storage properties of Mg nanocrystals prepared from solution. J. Am. Chem. Soc. **133**(28), 10679–10681 (2011). https://doi.org/10.1021/ja201791y
45. M. Konarova, A. Tanksale, J. Norberto Beltramini, G. Qing Lu, Effects of nano-confinement on the hydrogen desorption properties of MgH_2. Nano Energy **2**(1), 98–104 (2013)
46. C.J. Webb, A review of catalyst-enhanced magnesium hydride as a hydrogen storage material. J. Phys. Chem. Solids **84**, 96–106 (2015). https://doi.org/10.1016/j.jpcs.2014.06.014
47. A. Jain, S. Agarwal, T. Ichikawa, Catalytic tuning of sorption kinetics of lightweight hydrides: a review of the materials and mechanism. Catalysts **8**(12), 651 (2018). https://doi.org/10.3390/catal8120651
48. R. Bardhan, A.M. Ruminski, A. Brand, J.J. Urban, Magnesium nanocrystal-polymer composites: a new platform for designer hydrogen storage materials. Energy Environ. Sci. **4**(12), 4882–4895 (2011). https://doi.org/10.1039/C1EE02258J
49. E.A.V. Ebsworth, Hydrogen compounds of the metallic elements. J. Inorg. Nucl. Chem. **29**(7), 1823 (1967). https://doi.org/10.1016/0022-1902(67)80236-7
50. B. Bogdanović, K. Bohmhammel, B. Christ, A. Reiser, K. Schlichte et al., Thermodynamic investigation of the magnesium–hydrogen system. J. Alloys Compd. **282**(1), 84–92 (1999). https://doi.org/10.1016/S0925-8388(98)00829-9
51. K.-F. Aguey-Zinsou, J.-R. Ares-Fernández, Hydrogen in magnesium: new perspectives toward functional stores. Energy Environ. Sci. **3**(5), 526–543 (2010). https://doi.org/10.1039/B921645F
52. J. Zhang, Z. Li, Y. Wu, X. Guo, J. Ye et al., Recent advances on the thermal destabilization of Mg-based hydrogen storage materials. RSC Adv. **9**(1), 408–428 (2019). https://doi.org/10.1039/C8RA05596C
53. S. Cheung, W.-Q. Deng, A.C.T. van Duin, W.A. Goddard, $ReaxFF_{MgH}$ reactive force field for magnesium hydride systems. J. Phys. Chem. A **109**(5), 851–859 (2005). https://doi.org/10.1021/jp0460184
54. A. Gupta, G.V. Baron, P. Perreault, S. Lenaerts, R.-G. Ciocarlan et al., Hydrogen clathrates: next generation hydrogen storage materials. Energy Storage Mater. **41**, 69–107 (2021). https://doi.org/10.1016/j.ensm.2021.05.044
55. M. Pezat, B. Darriet, P. Hagenmuller, A comparative study of magnesium-rich rare-earth-based alloys for hydrogen storage. J. Less-Common Met. **74**(2), 427–434 (1980). https://doi.org/10.1016/0022-5088(80)90181-2
56. J.F. Fernández, C.R. Sánchez, Rate determining step in the absorption and desorption of hydrogen by magnesium. J. Alloys Compd. **340**(1), 189–198 (2002). https://doi.org/10.1016/S0925-8388(02)00120-2
57. P. Spatz, H.A. Aebischer, A. Krozer, L. Schlapbach, The diffusion of H in Mg and the nucleation and growth of MgH_2 in thin films. Z. Phys. Chem. **181**(1–2), 393–397 (1993). https://doi.org/10.1524/zpch.1993.181.Part_1_2.393
58. H.T. Uchida, S. Wagner, M. Hamm, J. Kürschner, R. Kirchheim et al., Absorption kinetics and hydride formation in magnesium films: effect of driving force revisited. Acta Mater. **85**, 279–289 (2015). https://doi.org/10.1016/j.actamat.2014.11.031
59. V.A. Yartys, M.V. Lototskyy, E. Akiba, R. Albert, V.E. Antonov et al., Magnesium based materials for hydrogen based energy storage: past, present and future. Int. J. Hydrogen Energy **44**(15), 7809–7859 (2019). https://doi.org/10.1016/j.ijhydene.2018.12.212
60. R.A. Varin, T. Czujko, Z. Wronski, Particle size, grain size and γ-MgH_2 effects on the desorption properties of nanocrystalline commercial magnesium hydride processed by controlled mechanical milling. Nanotechnology **17**(15), 3856–3865 (2006). https://doi.org/10.1016/j.actamat.2022.118654
61. G. Barkhordarian, T. Klassen, R. Bormann, Kinetic investigation of the effect of milling time on the hydrogen sorption reaction of magnesium catalyzed with different Nb_2O_5 contents. J. Alloys Compd. **407**(1), 249–255 (2006). https://doi.org/10.1016/j.jallcom.2005.05.037
62. P.S. Rudman, Hydriding and dehydriding kinetics. J. Less-Common Met. **89**(1), 93–110 (1983). https://doi.org/10.1016/0022-5088(83)90253-9

 https://doi.org/10.1007/s40820-023-01041-5

63. Y. Pang, Q. Li, A review on kinetic models and corresponding analysis methods for hydrogen storage materials. Int. J. Hydrogen Energy **41**(40), 18072–18087 (2016). https://doi.org/10.1016/j.ijhydene.2016.08.018
64. M.H. Mintz, Y. Zeiri, Hydriding kinetics of powders. J. Alloys Compd. **216**(2), 159–175 (1995). https://doi.org/10.1016/0925-8388(94)01269-N
65. L. Mooij, B. Dam, Nucleation and growth mechanisms of nano magnesium hydride from the hydrogen sorption kinetics. Phys. Chem. Chem. Phys. **15**(27), 11501–11510 (2013). https://doi.org/10.1039/C3CP51735G
66. H.E. Kissinger, Reaction kinetics in differential thermal analysis. Anal. Chem. **29**(11), 1702–1706 (1957). https://doi.org/10.1021/ac60131a045
67. T. Huang, H. Liu, C. Zhou, Effect of driving force on the activation energies for dehydrogenation and hydrogenation of catalyzed MgH_2. Int. J. Hydrogen Energy **46**(76), 37986–37994 (2021). https://doi.org/10.1016/j.ijhydene.2021.09.044
68. R.W.P. Wagemans, J.H. van Lenthe, P.E. de Jongh, A.J. van Dillen, K.P. de Jong, Hydrogen storage in magnesium clusters: quantum chemical study. J. Am. Chem. Soc. **127**(47), 16675–16680 (2005). https://doi.org/10.1021/ja054569h
69. C. Hu, Z. Zheng, T. Si, Q. Zhang, Enhanced hydrogen desorption kinetics and cycle durability of amorphous $TiMgVNi_3$-doped MgH_2. Int. J. Hydrogen Energy **47**(6), 3918–3926 (2022). https://doi.org/10.1016/j.ijhydene.2021.11.010
70. C. Peng, Y. Li, Q. Zhang, Enhanced hydrogen desorption properties of MgH_2 by highly dispersed Ni: the role of in-situ hydrogenolysis of nickelocene in ball milling process. J. Alloys Compd. **900**, 163547 (2022). https://doi.org/10.1016/j.jallcom.2021.163547
71. Y. Fu, L. Zhang, Y. Li, S. Guo, Z. Yu et al., Catalytic effect of MOF-derived transition metal catalyst FeCoS@C on hydrogen storage of magnesium. J. Mater. Sci. Technol. **138**, 59–69 (2023). https://doi.org/10.1016/j.jmst.2022.08.019
72. M. Felderhoff, B. Bogdanović, High temperature metal hydrides as heat storage materials for solar and related applications. Int. J. Hydrogen Energy **10**(1), 325–344 (2009). https://doi.org/10.3390/ijms10010325
73. L.Z. Ouyang, S.Y. Ye, H.W. Dong, M. Zhu, Effect of interfacial free energy on hydriding reaction of Mg–Ni thin films. Appl. Phys. Lett. **90**(2), 021917 (2007). https://doi.org/10.1063/1.2428877
74. Y. Jia, C. Sun, S. Shen, J. Zou, S.S. Mao et al., Combination of nanosizing and interfacial effect: future perspective for designing Mg-based nanomaterials for hydrogen storage. Renew. Sustain. Energy Rev. **44**, 289–303 (2015). https://doi.org/10.1016/j.rser.2014.12.032
75. K.-F. Aguey-Zinsou, J.-R. Ares-Fernández, Synthesis of colloidal magnesium: a near room temperature store for hydrogen. Chem. Mater. **20**, 376 (2008). https://doi.org/10.1021/cm702897f
76. W. Li, C. Li, C. Zhou, H. Ma, J. Chen, Metallic magnesium nano/mesoscale structures: their shape-controlled preparation and Mg/Air battery applications. Angew. Chem. Int. Ed. **45**(36), 6009–6012 (2006). https://doi.org/10.1002/anie.200600099
77. W.Y. Li, C.S. Li, H. Ma, J. Chen, Magnesium nanowires: enhanced kinetics for hydrogen absorption and desorption. J. Am. Chem. Soc. **129**(21), 6710–6711 (2007). https://doi.org/10.1021/ja071323z
78. X. Zhang, Y. Liu, Z. Ren, X. Zhang, J. Hu et al., Realizing 6.7 wt% reversible storage of hydrogen at ambient temperature with non-confined ultrafine magnesium hydrides. Energy Environ. Sci. **14**, 2302–2313 (2021). https://doi.org/10.1039/D0EE03160G
79. J. Huot, G. Liang, S. Boily, A. Van Neste, R. Schulz, Structural study and hydrogen sorption kinetics of ball-milled magnesium hydride. J. Alloys Compd. **293**, 495–500 (1999). https://doi.org/10.1016/S0925-8388(99)00474-0
80. G. Liang, J. Huot, S. Boily, A. Van Neste, R. Schulz, Catalytic effect of transition metals on hydrogen sorption in nanocrystalline ball milled MgH_2–Tm (Tm=Ti, V, Mn, Fe and Ni) systems. J. Alloys Compd. **292**(1), 247–252 (1999). https://doi.org/10.1016/S0925-8388(99)00442-9
81. J.L. Bobet, E. Akiba, Y. Nakamura, B. Darriet, Study of Mg–M (M = Co, Ni and Fe) mixture elaborated by reactive mechanical alloying—hydrogen sorption properties. Int. J. Hydrog. Energy **25**(10), 987–996 (2000). https://doi.org/10.1016/s0360-3199(00)00002-1
82. N. Hanada, T. Ichikawa, H. Fujii, Catalytic effect of nanoparticle 3d-transition metals on hydrogen storage properties in magnesium hydride MgH_2 prepared by mechanical milling. J. Phys. Chem. B **109**(15), 7188–7194 (2005). https://doi.org/10.1021/jp044576c
83. L. Dan, H. Wang, J. Liu, L. Ouyang, M. Zhu, H_2 plasma reducing Ni nanoparticles for superior catalysis on hydrogen sorption of MgH_2. ACS Appl. Mater. Interfaces **5**(4), 4976–4984 (2022). https://doi.org/10.1021/acsaem.2c00206
84. X. Lu, L. Zhang, H. Yu, Z. Lu, J. He et al., Achieving superior hydrogen storage properties of MgH_2 by the effect of TiFe and carbon nanotubes. Chem. Eng. J. **422**, 130101 (2021). https://doi.org/10.1016/j.cej.2021.130101
85. K. Wang, X. Zhang, Y. Liu, Z. Ren, X. Zhang et al., Graphene-induced growth of *N*-doped niobium pentaoxide nanorods with high catalytic activity for hydrogen storage in MgH_2. Chem. Eng. J. **406**, 126831 (2021). https://doi.org/10.1016/j.cej.2020.126831
86. K.C. Tome, S. Xi, Y. Fu, C. Lu, N. Lu et al., Remarkable catalytic effect of Ni and ZrO_2 nanoparticles on the hydrogen sorption properties of MgH_2. Int. J. Hydrogen Energy **47**(7), 4716–4724 (2022). https://doi.org/10.1016/j.ijhydene.2021.11.102
87. N.S. Mustafa, M. Ismail, Hydrogen sorption improvement of MgH_2 catalyzed by CeO_2 nanopowder. J. Alloys Compd. **695**, 2532–2538 (2017). https://doi.org/10.1016/j.jallcom.2016.11.158
88. A. Bhatnagar, S.K. Pandey, A.K. Vishwakarma, S. Singh, V. Shukla et al., Fe_3O_4@graphene as a superior catalyst for hydrogen de/absorption from/in MgH_2/Mg. J. Mater. Chem.

A **4**(38), 14761–14772 (2016). https://doi.org/10.1039/C6TA05998H

89. C. Peng, C. Yang, Q. Zhang, Few-layer MXene $Ti_3C_2T_x$ supported Ni@C nanoflakes as a catalyst for hydrogen desorption of MgH_2. J. Mater. Chem. A **10**(23), 12409–12417 (2022). https://doi.org/10.1039/D2TA02958H
90. Z. Lan, H. Fu, R. Zhao, H. Liu, W. Zhou et al., Roles of in situ-formed NbN and Nb_2O_5 from *N*-doped Nb_2C MXene in regulating the re/hydrogenation and cycling performance of magnesium hydride. Chem. Eng. J. **431**, 133985 (2022). https://doi.org/10.1016/j.cej.2021.133985
91. H. Liu, C. Lu, X. Wang, L. Xu, X. Huang et al., Combinations of V_2C and Ti_3C_2 MXenes for boosting the hydrogen storage performances of MgH_2. ACS Appl. Mater. Interfaces **13**(11), 13235–13247 (2021). https://doi.org/10.1021/acsami.0c23150
92. G. Haiguang, S. Rui, Z. Jinglian, L. Yana, S. Yuting et al., Interface effect in sandwich like Ni/Ti_3C_2 catalysts on hydrogen storage performance of MgH_2. Appl. Surf. Sci. **564**, 150302 (2021). https://doi.org/10.1016/j.apsusc.2021.150302
93. G. Haiguang, S. Yuting, S. Rui, L. Yana, Z. Jinglian et al., Effect of few-layer $Ti_3C_2T_x$ supported nano-Ni via self-assembly reduction on hydrogen storage performance of MgH_2. ACS Appl. Mater. Interfaces **564**, 150302 (2021). https://doi.org/10.1021/acsami.0c15686
94. K. Wang, X. Zhang, Z. Ren, X. Zhang, J. Hu et al., Nitrogen-stimulated superior catalytic activity of niobium oxide for fast full hydrogenation of magnesium at ambient temperature. Energy Storage Mater. **23**, 79–87 (2019). https://doi.org/10.1016/j.ensm.2019.05.029
95. W. Oelerich, T. Klassen, R. Bormann, Comparison of the catalytic effects of V, V_2O_5, VN, and VC on the hydrogen sorption of nanocrystalline Mg. J. Alloys Compd. **322**(1–2), L5–L9 (2001). https://doi.org/10.1016/s0925-8388(01)01173-2
96. A.R. Yavari, A. LeMoulec, F.R. de Castro, S. Deledda, O. Friedrichs et al., Improvement in H-sorption kinetics of MgH_2 powders by using Fe nanoparticles generated by reactive FeF_3 addition. Scr. Mater. **52**(8), 719–724 (2005). https://doi.org/10.1016/j.scriptamat.2004.12.020
97. M. Liu, X. Xiao, S. Zhao, M. Chen, J. Mao et al., Facile synthesis of Co/Pd supported by few-walled carbon nanotubes as an efficient bidirectional catalyst for improving the low temperature hydrogen storage properties of magnesium hydride. J. Mater. Chem. A **7**(10), 5277–5287 (2019). https://doi.org/10.1039/C8TA12431K
98. J. Zang, S. Wang, R. Hu, H. Man, J. Zhang et al., Ni, beyond thermodynamic tuning, maintains the catalytic activity of V species in $Ni_3(VO_4)_2$ doped MgH_2. J. Mater. Chem. A **9**(13), 8341–8349 (2021). https://doi.org/10.1039/d0ta12079k
99. T. Huang, X. Huang, C. Hu, J. Wang, H. Liu et al., Enhancing hydrogen storage properties of MgH_2 through addition of Ni/$CoMoO_4$ nanorods. Mater. Today Energy **19**, 100613 (2021). https://doi.org/10.1016/j.mtener.2020.100613
100. K. Xian, M. Wu, M. Gao, S. Wang, Z. Li et al., A unique nanoflake-shape bimetallic Ti–Nb oxide of superior catalytic effect for hydrogen storage of MgH_2. Small **18**(43), 2107013 (2022). https://doi.org/10.1002/smll.202107013
101. X. Wen, H. Liang, R. Zhao, F. Hong, W. Shi et al., Regulation of the integrated hydrogen storage properties of magnesium hydride using 3D self-assembled amorphous carbon-embedded porous niobium pentoxide. J. Mater. Chem. A **10**(32), 16941–16951 (2022). https://doi.org/10.1039/D2TA04700D
102. W. Zhu, S. Panda, C. Lu, Z. Ma, D. Khan et al., Using a self-assembled two-dimensional MXene-based catalyst (2D-Ni@Ti_3C_2) to enhance hydrogen storage properties of MgH_2. ACS Appl. Mater. Interfaces **12**(45), 50333–50343 (2020). https://doi.org/10.1021/acsami.0c12767
103. H. Tianping, H. Xu, H. Chuanzhu, W. Jie, L. Huabing et al., MOF-derived Ni nanoparticles dispersed on monolayer MXene as catalyst for improved hydrogen storage kinetics of MgH_2. Chem. Eng. J. **421**, 127851 (2021). https://doi.org/10.1016/j.cej.2020.127851
104. M. Liu, X. Xiao, S. Zhao, S. Saremi-Yarahmadi, M. Chen et al., ZIF-67 derived Co@CNTs nanoparticles: remarkably improved hydrogen storage properties of MgH_2 and synergetic catalysis mechanism. Int. J. Hydrog. Energy **44**(2), 1059–1069 (2019). https://doi.org/10.1016/j.ijhydene.2018.11.078
105. L. Ouyang, Z. Cao, H. Wang, R. Hu, M. Zhu, Application of dielectric barrier discharge plasma-assisted milling in energy storage materials—a review. J. Alloys Compd. **691**, 422–435 (2017). https://doi.org/10.1016/j.jallcom.2016.08.179
106. L.Z. Ouyang, Z.J. Cao, H. Wang, J.W. Liu, D.L. Sun et al., Enhanced dehydriding thermodynamics and kinetics in Mg(In)–MgF_2 composite directly synthesized by plasma milling. J. Alloys Compd. **586**, 113–117 (2014). https://doi.org/10.1016/j.jallcom.2013.10.029
107. J. Cui, J. Liu, H. Wang, L. Ouyang, D. Sun et al., Mg–TM (TM: Ti, Nb, V Co, Mo or Ni) core–shell like nanostructures: synthesis, hydrogen storage performance and catalytic mechanism. J. Mater. Chem. A **2**(25), 9645–9655 (2014). https://doi.org/10.1039/c4ta00221k
108. C. Jie, W. Hui, L. Jiangwen, O. Liuzhang, Z. Qingan et al., Remarkable enhancement in dehydrogenation of MgH_2 by a nano-coating of multi-valence Ti-based catalysts. J. Mater. Chem. A **1**(18), 5603–5611 (2013). https://doi.org/10.1039/c3ta01332d
109. C. Lu, J. Zou, X. Shi, X. Zeng, W. Ding, Synthesis and hydrogen storage properties of core–shell structured binary Mg@Ti and ternary Mg@Ti@Ni composites. Int. J. Hydrog. Energy **42**(4), 2239–2247 (2017). https://doi.org/10.1016/j.ijhydene.2016.10.088
110. C. Lu, Y. Ma, F. Li, H. Zhu, X. Zeng et al., Visualization of fast "hydrogen pump" in core–shell nanostructured Mg@Pt through hydrogen-stabilized Mg_3Pt. J. Mater. Chem. A **7**(24), 14629–14637 (2019). https://doi.org/10.1039/c9ta03038g
111. A. Schneemann, J.L. White, S. Kang, S. Jeong, L.F. Wan et al., Nanostructured metal hydrides for hydrogen storage.

 https://doi.org/10.1007/s40820-023-01041-5

Chem. Rev. **118**(22), 10775–10839 (2018). https://doi.org/10.1021/acs.chemrev.8b00313

112. A.G. Turnbull, Thermochemistry of biscyclopentadienyl metal compounds. Aust. J. Chem. **20**(10), 2059–2067 (1967). https://doi.org/10.1071/CH9672059
113. J.-J. Liang, W.C.P. Kung, Confinement of Mg–MgH_2 systems into carbon nanotubes changes hydrogen sorption energetics. J. Phys. Chem. B **109**(38), 17837–17841 (2005). https://doi.org/10.1021/jp052134a
114. P.E. de Jongh, R.W.P. Wagemans, T.M. Eggenhuisen, B.S. Dauvillier, P.B. Radstake et al., The preparation of carbon-supported magnesium nanoparticles using melt infiltration. Chem. Mater. **19**(24), 6052–6057 (2007). https://doi.org/10.1021/cm702205v
115. M. Liu, S. Zhao, X. Xiao, M. Chen, C. Sun et al., Novel 1D carbon nanotubes uniformly wrapped nanoscale MgH_2 for efficient hydrogen storage cycling performances with extreme high gravimetric and volumetric capacities. Nano Energy **61**, 540–549 (2019). https://doi.org/10.1016/j.nanoen.2019.04.094
116. G. Xia, Y. Tan, X. Chen, D. Sun, Z. Guo et al., Monodisperse magnesium hydride nanoparticles uniformly self-assembled on graphene. Adv. Mater. **27**(39), 5981–5988 (2015). https://doi.org/10.1002/adma.201502005
117. W. Zhu, L. Ren, C. Lu, H. Xu, F. Sun et al., Nanoconfined and in situ catalyzed MgH_2 self-assembled on 3D Ti_3C_2 MXene folded nanosheets with enhanced hydrogen sorption performances. ACS Nano **15**(11), 18494–18504 (2021). https://doi.org/10.1021/acsnano.1c08343
118. S. Liu, J. Liu, X. Liu, J. Shang, L. Xu et al., Hydrogen storage in incompletely etched multilayer Ti_2CT_x at room temperature. Nat. Nanotechnol. **16**, 331–336 (2021). https://doi.org/10.1038/s41565-020-00818-8
119. M. Naguib, M. Kurtoglu, V. Presser, J. Lu, J. Niu et al., Two-dimensional nanocrystals produced by exfoliation of Ti_3AlC_2. Adv. Mater. **23**(37), 4248–4253 (2011). https://doi.org/10.1002/adma.201102306
120. P. Kumar, S. Singh, S.A.R. Hashmi, K.-H. Kim, MXenes: emerging 2D materials for hydrogen storage. Nano Energy **85**, 105989 (2021). https://doi.org/10.1016/j.nanoen.2021.105989
121. D.W. Lim, J.W. Yoon, K.Y. Ryu, M.P. Suh, Magnesium nanocrystals embedded in a metal–organic framework: hybrid hydrogen storage with synergistic effect on physi- and chemisorption. Angew. Chem. Int. Ed. **51**(39), 9814–9817 (2012). https://doi.org/10.1002/anie.201206055
122. S.S. Shinde, D.-H. Kim, J.-Y. Yu, J.-H. Lee, Self-assembled air-stable magnesium hydride embedded in 3-D activated carbon for reversible hydrogen storage. Nanoscale **9**(21), 7094–7103 (2017). https://doi.org/10.1039/C7NR01699A
123. Z. Ma, S. Panda, Q. Zhang, F. Sun, D. Khan et al., Improving hydrogen sorption performances of MgH_2 through nanoconfinement in a mesoporous CoS nano-boxes scaffold. Chem. Eng. J. **406**, 126790 (2021). https://doi.org/10.1016/j.cej.2020.126790
124. L. Ren, W. Zhu, Y. Li, X. Lin, H. Xu et al., Oxygen vacancy-rich 2D TiO_2 nanosheets: a bridge toward high stability and rapid hydrogen storage kinetics of nano-confined MgH_2. Nano-Micro Lett. **14**(1), 144 (2022). https://doi.org/10.1007/s40820-022-00891-9
125. Z. Ma, Q. Zhang, S. Panda, W. Zhu, F. Sun et al., In situ catalyzed and nanoconfined magnesium hydride nanocrystals in a Ni–MOF scaffold for hydrogen storage. Sustain. Energy Fuels **4**(9), 4694–4703 (2020). https://doi.org/10.1039/D0SE00818D
126. T. Qiu, S. Gao, Z. Liang, D.G. Wang, H. Tabassum et al., Pristine hollow metal–organic frameworks: design, synthesis and application. Angew. Chem. Int. Ed. **60**, 17314 (2021). https://doi.org/10.1002/anie.202012699
127. L. Ren, W. Zhu, Q. Zhang, C. Lu, F. Sun et al., MgH_2 confinement in MOF-derived *N*-doped porous carbon nanofibers for enhanced hydrogen storage. Chem. Eng. J. **434**, 134701 (2022). https://doi.org/10.1016/j.cej.2022.134701
128. M. Huang, L. Ouyang, J. Ye, J. Liu, X. Yao et al., Hydrogen generation via hydrolysis of magnesium with seawater using Mo, MoO_2, MoO_3 and MoS_2 as catalysts. J. Mater. Chem. A **5**(18), 8566–8575 (2017). https://doi.org/10.1039/C7TA02457F
129. Y. Zhao, T. Li, H. Huang, T. Xu, B. Liu et al., A highly efficient hydrolysis of MgH_2 catalyzed by NiCo@C bimetallic synergistic effect. J. Mater. Sci. Technol. **137**, 176–183 (2023). https://doi.org/10.1016/j.jmst.2022.08.005
130. M. Song, L. Zhang, F. Wu, H. Zhang, H. Zhao et al., Recent advances of magnesium hydride as an energy storage material. J. Mater. Sci. Technol. **149**, 99–111 (2023). https://doi.org/10.1016/j.jmst.2022.11.032
131. L. Ouyang, W. Chen, J. Liu, M. Felderhoff, H. Wang et al., Enhancing the regeneration process of consumed $NaBH_4$ for hydrogen storage. Adv. Energy Mater. **7**(19), 1700299 (2017). https://doi.org/10.1002/aenm.201700299
132. Y. Zhu, L. Ouyang, H. Zhong, J. Liu, H. Wang et al., Closing the loop for hydrogen storage: facile regeneration of $NaBH_4$ from its hydrolytic product. Angew. Chem. Int. Ed. **59**(22), 8623–8629 (2020). https://doi.org/10.1002/anie.201915988
133. K. Chen, L. Ouyang, H. Zhong, J. Liu, H. Wang et al., Converting H^+ from coordinated water into H^- enables super facile synthesis of $LiBH_4$. Green Chem. **21**(16), 4380–4387 (2019). https://doi.org/10.1039/C9GC01897B
134. P. Gao, S. Ju, Z. Liu, G. Xia, D. Sun et al., Metal hydrides with in situ built electron/ion dual-conductive framework for stable all-solid-state Li-ion batteries. ACS Nano **16**(5), 8040–8050 (2022). https://doi.org/10.1021/acsnano.2c01038
135. H. Zhang, Y. Wang, S. Ju, P. Gao, T. Zou et al., 3D artificial electron and ion conductive pathway enabled by MgH_2 nanoparticles supported on g-C_3N_4 towards dendrite-free Li metal anode. Energy Storage Mater. **52**, 220–229 (2022). https://doi.org/10.1016/j.ensm.2022.08.001
136. S. Zhong, S. Ju, Y. Shao, W. Chen, T. Zhang et al., Magnesium hydride nanoparticles anchored on MXene sheets as high capacity anode for lithium-ion batteries. J. Energy Chem. **62**, 431–439 (2021). https://doi.org/10.1016/j.jechem.2021.03.049